A Novel Multi-Layer Framework for Dynamic Operation of Prosumers in Peer-to-Peer (P2P) Energy Markets

by

Muhammad Umar Azam

A thesis
presented to the University of Waterloo
in fulfillment of the
thesis requirement for the degree of
Master of Applied Science
in
Electrical & Computer Engineering

Waterloo, Ontario, Canada, 2020

Author's Declaration

I hereby declare that I am the sole author of this thesis. This is a true copy of the thesis, including any required final revisions, as accepted by my examiners.

I understand that my thesis may be made electronically available to the public.

Abstract

Research in transactive energy systems, in recent years, has been primarily focused on the financial aspects of peer-to-peer (P2P) energy trade with little attention paid to the operational and practical aspects of how this energy trade should occur in a system. Practical prosumer behavior in such systems should be subject to their own internal status and the external conditions of the electrical network. Moreover, for such practical realization of a prosumer to be feasible, they should be primed to operate through system disturbances and parameter uncertainties.

In this thesis, a novel mathematical model is presented to enable prosumers to partake in P2P energy trades with full operational freedom over their own consumption, energy storage system (ESS) operation and their distributed power generation capability. The proposed model integrates a physical system (physical layer) with prosumer operations (virtual layer) to evolve a multi-layer framework which allows physical network constraints to be implemented with relative ease. The formulation is implemented on a 33-Bus test system considering various system objectives and the results demonstrably prove the significance and applicability of the proposed framework in P2P energy markets.

The multi-layer framework is then further extended to enable the prosumer to respond to uncertainties in the local grid or its distributed energy resources, through an MPC based approach. The considered uncertainties are further split into categories termed as 'known uncertainty' and 'unknown uncertainty'; with the former referring to forecasting errors and the latter referring to unexpected system disturbances. Several cases are developed considering combinations of system parameters to be uncertain and by introducing disturbances to observe prosumer responses. The simulation results prominently show the prosumers responding to unexpected disturbances by adjusting their behavior and P2P energy trade while maintaining their optimal objectives. Such results demonstrate the viability of this MPC approach for the realization of a practical prosumer.

Acknowledgements

I would like to express my heartfelt gratitude to all the people who have contributed, directly and indirectly, to the completion of this thesis.

Foremost, I would thank my supervisor, Professor Kankar Bhattacharya, for his continuous support and guidance throughout my master's studies. It has been an immensely rewarding experience to learn the art of research, and to complete this degree under his tutelage.

I would like to acknowledge Professor Sagar Naik and Professor Mohammed Nassar for volunteering to serve as members of my thesis committee. Their comments and inputs on the content of this thesis are greatly appreciated.

Special thanks to the Natural Sciences and Engineering Research Council of Canada (NSERC), and the University of Waterloo, for the financial and academic support provided over the course of this degree.

I would also like to thank my friends, Omar Alrumayh and Talal Alharbi, for all the help and support they have offered over the course of my research.

My greatest gratitude is extended to my parents, to my mother Atia, and to my father Muhammad, for their prayers and moral support through the trials and challenges of my graduate studies. And to my siblings for their encouragement and humor, which has helped me during my stay in Canada.

Dedication

Dedicated to my lovely mother, Atia, my amazing father Muhammad, and my awesome siblings, Haider, Taimoor, and Zainab.

Table of Contents

List of Figures

List of Tables

Nomenclature

Indices and Sets

i, j Index of prosumers $i, j \in \mathcal{N}$

bi, bj Index of buses in the system $bi, bj \in \mathcal{B}$

t, tt, tf Index of time slots $t \in \mathcal{T}$

Parameters

$C_{i,bi}^{LOC}$ Incidence matrix for prosumer location.

$D_{i,t}^{\max}, D_{i,t}^{\min}$ Prosumer upper/lower consumption, kW

$E_i^{\max}, E_i^{\min}$ ESS upper/lower SOC limit, kWh

$P_{bi,t}^{load}$ Real non-participating load, kW

$P_i^{Ch_{\max}}, P_i^{Dch_{\max}}$ ESS max charging/discharging power, kW

$P_{i,t}^{PV}$ Photovoltaic power available, kW

$Q_{bi,t}^{load}$ Reactive non-participating load, kVAr

S_{base} Base Power for load flow equations, kVA

$Y_{bi,bj}$ Admittance matrix magnitude element, pu

$\phi_{bi,bj}$ Admittance matrix element phase, pu

$\eta_i^{Ch}, \eta_i^{Dch}$ ESS charging/discharging efficiency

$\alpha_{i,t}, \beta_i$ Prosumer utility function parameters

π_t^{G2P} Price : buying power from grid \$/kWh

π_t^{P2G} Price : selling power to the grid, \$/kWh

π_t^{P2P} Price of power in the P2P market, \$/kWh

$\mathbb{M}$ Large number

Variables

$b_{i,t}^{Ch}, b_{i,t}^{Dch}$ Binary variables indicating prosumer ESS charing/discharging state

$E_{i,t}$ Prosumer ESS state of charge, kWh

$P_{i,t}^{Ch}, P_{i,t}^{Dch}$ Prosumer ESS charging/discharing, kW

$P_{i,t}^{P2G}$ Power sold to grid by the prosumer, kW

$P_{i,t}^{G2P}$ Power sold to Prosumer by the grid, kW

$s_{i,t}$ Binary variable indicating status of a prosumer [1 = seller, 0 = buyer]

$V_{bi,t}$ Bus voltage magnitude, pu

$x_{i,t}$ Prosumer power consumption, kW

$x_{j,i,t}^{P2P}$ Power sold in P2P market by prosumer j to prosumer i at time t, kW

$\theta_{bi,t}$ Bus voltage phase, rad

Chapter 1

Introduction

1.1 Motivation

The traditional electricity markets have undergone a shift in recent years with the advent and increasing penetration of Distributed Energy Resources (DERs) and intelligent loads. This shift has seen the role of the consumers become flexible, with greater control over their consumption and the ability to act either as a load or even a producer. The consumers that possess this flexibility are referred to as 'prosumers' [1] and have the ability to trade energy amongst themselves, in what is called, a peer-to-peer (P2P) energy market. This P2P energy market is an emerging concept called Transactive Energy [2] which has become a prominent topic of research in recent literature. The emergence of this concept can be attributed to advancements in intercommunication, self-awareness and self-control among entities engaged with the power network. Such features collectively fall under the paradigm of a smart grid [3] and enable the design and implementation of strategies that can improve grid stability, reliability and efficiency, while considering consumer welfare, as well. This is a win-win scenario and is the main motivation behind the advancement of transactive energy technologies. P2P energy trading generalizes the roles of sellers and buyers, and expands the possible financial structures that can be used in this new paradigm.

Most of the research content in the domain of P2P energy trade can be split into two categories or layers [4]. The first is the virtual layer which has received most of the attention from researchers; it primarily deals with the financial and operational management of prosumers in the P2P market, i.e., managing prosumer energy resources, P2P energy pricing, P2P energy market operations, etc. The second is the physical layer which deals with the physical status, parameters of the electrical network and grid interface of prosumers;

this layer has not been well explored so far. The published literature encompasses either one or both of these layers with varying degrees of development in each. This thesis aims to address both.

As the availability of privately owned DERs becomes increasingly commonplace in the electricity grid, there is a notable scarcity of strategies and systems to proactively utilize these new resources (DERs) for the maximum benefit of prosumers that own them and the grid hosting these prosumers. This proactive operation is indicative of a 'smarter' class of prosumers whose behavior is more deeply intertwined with that of the grid, and their actions actively conforming to physical grid limitations and contributing to grid stability; while the grid operator can influence and direct the decisions made by the prosumer. While each of these topics have been separately explored in the literature, they are rarely tackled together and even then the prosumer behaviors are restricted. The impact of operational freedom of prosumers needs to be explored at length.

The flexibility that prosumers introduce by adjusting their power exchange with the grid (which is significantly higher when they possess an Energy Storage System) is increasing and enables contribution towards grid support functions and in order to leverage these supportive functions, the impact of prosumer operations on the physical system must be evaluated as well. Such a cohesive response from prosumers can be a valuable tool for increasing grid stability (by helping maintain system bus voltages/system frequency).

The operational freedom of prosumers is one of the two aspects of their dynamic operation; the other being their response to forecastable and unforecastable uncertainties. In order for the prosumer to make optimal decisions, the forecasts of some parameters are required. These parameters include but are not limited to PV generation, electricity costs, prosumer demand, etc. These forecasts are not accurate, however, and some unexpected deviations can occur which the dynamic prosumer should be able to respond to actively while maintaining its overall objective. This feature of prosumer 'alertness' needs to be explored further since it pertains to real world eventualities which remain unaddressed.

1.2 Literature Review

The topic of transactive energy is currently a highly active one, in terms of research output. In the context of the P2P virtual layer, it is noted that works reported in the literature on optimal P2P energy trade primarily draw influence from economic strategies. Stackelberg games and auction theory are some commonly used approaches in this domain. In several of the works, optimization problems are developed to obtain optimal prosumer operational

decisions in the P2P market. The optimization approach is used in both layers, where in the virtual layer it is used for welfare maximization and cost minimization, while in the physical layer for optimal power routing.

1.2.1 Peer-to-Peer Energy Trade

A cooperative Stackelberg game is developed in [5] where the centralized power system acts as a leader to decide a price and the prosumers act as followers to form coalitions to trade energy among themselves. The idea behind this approach is to enable the grid to the peak power pricing as an economic signal to incentivize the prosumers to lower their dependence on the grid by engaging in P2P trade. The energy surplus and deficit of prosumers engaging in P2P energy trade is statically determined and their roles are fixed for participation in the Stackelberg game. The work in this paper is entirely in the domain of the virtual layer and there is no focus on a practical implementation in physical systems.

In [6] a similar Stackelberg game is developed where a P2P market operator acts as a leader and the prosumers act as followers to select an energy sharing region similar to the coalition formation strategy of [5]. There is some focus on the physical layer in this case, through the use of linear power flow equations. It is assumed that a distribution system operator (DSO) has the responsibility of informing the P2P market operator of any line overload; where upon such a warning, additional power flow constraints are added to the system. The system voltages and losses are not considered in this paper and the responsibility of managing such variables is delegated to the DSO.

In contrast to [5] and [6], in [7] the prosumers with an energy surplus (Sellers) act as leaders and prosumers with an energy deficit (Buyers) act as followers. In addition to the Stackelberg game, there is a non-cooperative game for sellers to decide their price and an evolutionary game for buyers to select sellers. One notable issue in such an approach is that of scalability; since an increasing number of prosumers will slow down the convergence significantly. Furthermore, the prosumer participation roles for P2P trade are predetermined through a generation-to-demand ratio (GDR) and are fixed for a particular interval. The scope of this work is entirely within the virtual layer.

A Stackelberg game similar to [7] is used in [8] to model the interactions between buyers and sellers. Here again, the prosumers with surplus energy act as leaders and prosumers with an energy deficit act as followers to participate in P2P energy trade. The energy to be traded among the prosumers is predetermined through a scheduling algorithm which effectively defines prosumers' roles for a given time interval. Consequently, this static prosumer behavior can not be extended to real-time operations. Line congestions

in the physical systems are handled by considering a congestion cost which affects the optimization function to alleviate congestion. The line losses are calculated using a power flow program which also determines where the congestion occurs so that a congestion cost can be assigned.

Similarly in [9], a multi-leader multi-follower Stackelberg game is developed where prosumers with energy surplus act as leaders and prosumers with an energy deficit act as buyers. Prosumers are clustered into virtual microgrids where they can engage in P2P energy trade with other prosumers in the cluster to maximize their collective social welfare. A clustering scheme is proposed that uses various communication technologies being used currently in the industry. However, the paper does not consider the physical layer aspects of the electrical network.

The work in [10] draws influence from networking and digital communication concepts to develop a P2P energy trading framework where energy is traded in discretized packets. A central power router is proposed which is used to run an iterative auction for P2P energy trade with the objective of maximizing prosumer revenues and utility. In order to participate in the auction the prosumers register themselves as buyers or sellers, hence their decision to select either role in this paper is static and not influenced by the system status and parameters (buying/selling prices, PV generation etc). This work is completely within the domain of the virtual layer and does not explore such P2P trades through a physical electrical network.

Another auction based approach is used in [11] where P2P energy trade is considered within the context of electric vehicles (EVs) and charging stations. A distinctive feature of this work is the application of a blockchain within a cluster of EVs (referred to in this paper as local aggregators) for the purpose of conducting financial transactions among the vehicles participating in energy trade. A satisfaction function is formulated to model the behavior of EVs within a cluster based on their battery energy levels and expected future usage. The aggregate of this utility for all the EVs and is then maximized using an iterative double auction algorithm to evaluate the energy exchanges in the cluster. The role of an EV in this study, as either a seller or a buyer is again decided by the EV itself based on its own preferences, effectively making it a predetermined static parameter in the P2P framework. The scope of this work does not extend to any physical considerations of power transfer in electrical systems.

An optimization problem is developed in [12] to evaluate the energy trade among prosumers participating in the P2P energy market. A welfare maxization approach is developed with the additional consideration of network losses and network utilization. Network losses are approximate considering the power exchanged through the grid, rather than ex-

act power flow equations, while the network utilization is evaluated through the use of power transfer distribution factors (PTDFs). This approximate approach towards some aspects of the physical electrical network is insufficient for the implementation of network constraints for voltage, power flow, etc. Again the roles of prosumers as either sellers or buyers in the P2P market are predetermined, similar to [11], where these roles are already decided when executing the optimization model.

A Mixed Integer Linear Programming (MILP) problem is formulated in [13] to minimize the net energy cost of a group of prosumers. The P2P market structure comprises a central entity is required for operational oversight and to conduct financial transactions between the prosumers. The prosumer operation in this paper however, is more flexible than most works discussed in this section, in that the model does not set prosumer behavior as a constant and allows them to act as buyers or sellers at any time interval. The optimal prosumer decisions are determined over an optimization horizon for which the electrical network is not considered. So the physical layer of prosumer operation here remains unaddressed. The centralized P2P market approach also contrasts with the distributed P2P market structures where the central computing system evaluates the prosumer decisions but the prosumers can conduct financial transactions themselves in a distributed manner; which is more suitable for use with distributed ledger and blockchain technologies.

An energy market is developed in [14] for P2P trade that factors in the usage and origin of the energy undergoing the P2P transaction. This is done by separating energy into different classes such as 'Green Energy' which is obtained from renewable energy sources, 'Subsidised Energy' which is low cost energy and 'Grid Energy' which is energy purchased from the grid. The reasoning behind the separation of energy into different classes is that prosumers can have varying behaviors due to which they can show preference to one class over the other. A P2P platform agent is modeled to set the P2P energy price and oversee the trade and hence the energy exchanges between different prosumers are not explicitly visible, similar to the model developed in [13]. In consideration of the electrical network, only the power loss between grid and distribution network is considered at the point of common coupling with an approximate expression. So this formulation cannot be directly employed when physical network constraints need to be enforced.

The role of market structures on the nature of P2P trade in a community microgrid, specifically in the context of energy storage is examined in [15]. The two structures proposed in this paper are for centralized and decentralized ESS operating in a microgrid. A P2P trading framework is then developed around these market structures and in the presence of PV generation, to minimize the prosumer operation cost over a time period. This model assumes power losses to be a fixed percentage of the energy being traded in the P2P market. While this approach simplifies the model complexity, it does so at the

cost of accuracy and potential prosumer participation in grid support functions.

The routing of electrical power through a physical network to minimize transmission losses, is one of the derivatives of the 'shortest path problem' applicable to research in power systems. A distributed optimization algorithm is formulated in [16] to evaluate the path with minimum power loss in a DC microgrid. The same problem is tackled in [17] as well, where a slime mould inspired algorithm is used to find this optimal route. Since the focus of both these papers is on routing, the surplus and deficit power at each bus is assumed to be fixed. Hence these works are entirely focused on the physical layer since prosumer operation and decisions are not considered to a significant degree in the problems.

A comprehensive formulation is developed in [18] for computationally fast P2P energy trade that also conforms to the physical network constraints. This is accomplished by grouping prosumers into a multi-level P2P market structure where prosumers can trade within their community on one level and communities can trade among themselves on another level. A distributed optimization problem is then developed to evaluate prosumer operation for maximum utility. A Network Utilization Charge (NUC) is introduced which affects prosumer behavior and decisions, and whose parameters are obtained by running a distribution load flow program. This charge is essentially a constraint violation cost similar to the congestion cost in [8], and ensures that P2P energy trade adheres to the physical system limits. This formulation requires an iterative operation oscillating between the optimization and load flow to ensure network compliance. Moreover, the prosumer behavior defined in this formulation is static where the decisions to buy and sell are clearly defined prior to participating in the P2P market.

A multi-layer framework is developed in [19] where a continuous double auction process is used to evaluate the P2P energy trade in a prosumer group, that complies with the electrical network constraints, and this is accomplished through a sensitivity coefficient based approach. The iterative model developed here delegates the responsibility of rapid state estimation using sensitivity coefficients, to the distribution system operator (DSO). The prosumers whose energy trade violates network constraints are subsequently barred by the DSO from participating in the P2P market. The obvious drawback of such a formulation is that the prosumer cannot be actively incentivized to provide grid support functions such as the loss minimization objective. Another aspect of prosumer behavior in this study is the static allocation of prosumer roles. Here the prosumers optimize their power consumption over the course of the day based on their own cost minimization objective and hence decide the amount of surplus or deficit for each interval of the horizon. This essentially fixes their roles and prevents them from making decisions for the benefit of the prosumer group as a whole or behaving dynamically in response to unpredictable variations in price or PV generation.

1.2.2 Application of Model Predictive Control to Uncertainty Analysis

The literature discussed above focused on various strategies employed to optimally conduct prosumer operations and energy transactions. These works do not comprehensively address the full scope of the prosumer's environment which often contains uncertainties in various system parameters. Model Predictive Control (MPC) is often used when dealing with uncertainties.

In [20] an MPC based approach is used to determine the battery ESS operations to meet the real-time mismatch between the day-ahead dispatch plan and power drawn by prosumers. The consumption of prosumers is considered to follow a forecasted profile with some uncertainty and randomness in small time intervals, which necessitates MPC application of ESS ensuring that the generation plan does not deviate from the optimized day-ahead generation schedule.

A Mixed Integer Linear Programming (MILP) formulation is developed in [21] which is coupled with an MPC approach for microgrid operations. The proposed formulation considers uncertainties in Renewable Energy Sources (RES), prosumer loads, and electricity prices, when executing an optimal power dispatch objective. A receding optimization horizon based MPC is considered to evaluate the optimal generation schedule and ESS usage. The study is conducted on a relatively small microgrid and assumes that no voltage, frequency or power constraints are being violated. This effectively limits the scalability of this approach because, as the size of the power network increases, the system physical constraint need to be considered.

An MPC based home energy management system is proposed in [22] which utilizes cloud technology for the processing and storage of prosumer/grid operational data. PV generation and prosumer demand forecasts are generated with some uncertainty and the developed formulation is optimized in the cloud to evaluate the optimal control decisions for load curtailment and ESS usage, while minimizing the overall operational system cost. It is to be noted that these decisions define the extent of prosumer capability effectively rendering this approach incompatible with P2P power exchange.

A home energy management system similar to [22] is developed in [23] focusing on the modeling and control of a consumer's devices. This paper considers the impact of uncertainties in PV generation and real time electricity prices on the optimal usage of major household appliances as well as an ESS while aiming to minimize power cost. The proposed MPC approach achieves a high temporal resolution without proportionally increasing the computational time by considering non-uniform time intervals.

In all the studies discussed above, the use of MPC in the context of optimal prosumer operation has been restricted to known uncertainties. While important system parameters (PV generation, prosumer demand, HOEP price, etc.) are forecastable to a significant degree of accuracy, their actual values may deviate significantly under the right circumstances, essentially catching a prosumer 'off guard'. These circumstances can range from unexpected clouds causing a severe dip in PV generation to a sudden loss of cheap generation resulting in the kick-in of expensive generation, thus creating a spike in the real-time market clearing price. These scenarios remain unexplored in the literature. Moreover, the physical nature of the electrical network is not taken into account in any of these works, which is required if the prosumer model considered in the MPC should adhere to system limits.

1.3 Research Objectives

In light of the discussions in Section 1.2, we note that operation of prosumers has been considerably restricted in the literature concerning P2P markets. Removing such restrictions to make them flexible, can not only improve prosumer welfare, but can also improve grid operation. However, such prosumer contribution towards grid support functions requires a physical layer model compatible with P2P energy trade. Based on the above discussions, the objectives of this thesis are as follows.

- Propose a novel and flexible multi-layer P2P energy trading framework that ensures compliance to physical network constraints and is compatible with any transactive energy strategy.
- Introduce a dynamic prosumer behavior model to enable greater operational freedom for prosumers. This behavior model is a part of the proposed multi-layer framework.
- Demonstrate through simulation studies as to how this dynamic prosumer behavior can be leveraged in order to improve system welfare.
- Embed the developed framework into an MPC based approach to enable prosumers to behave dynamically for both, expected and and unexpected uncertainties in the power system environment (consumption, generation, electricity pricing, etc.)

1.4 Thesis Outline

In Section 2, the theoretical basis of some of the concepts used in this thesis are discussed. The interpretation of a smart grid and a prosumer is first defined, followed by the details on the utility function and how it relates to prosumer satisfaction. The load flow integration into the proposed framework is briefly discussed, and finally a background to the MPC technique is presented. Section 3 introduces the detailed mathematical model of the proposed multi-layer framework along with the various objectives used to direct prosumer behavior. The model simulations for each of the objectives and discussions on their output conclude this chapter. The formulation developed in Chapter 3 is extended for an MPC application in Chapter 4 where the mathematical basis of this extension in addition to the details of new simulations are explained. Prosumer behavior in this MPC approach is then discussed under the various cases of uncertainties in prosumer/grid parameters. Finally Chapter 5 summarizes the notable contributions of the present work and identifies some of the possible future avenues of research.

Chapter 2

Background

In this chapter some of the ideas and concepts used in this thesis are explained in detail.

2.1 Smart Grid, the Prosumer, and Transactive Energy

The concept of a smart grid emerges from the increased capability of power generation/transmission & distribution/consumption entities to communicate with each other, to measure the state of their own operation, and to control these operations if the need arises [3]. The classical power system comprises the legacy grid and legacy consumers where there is no bidirectional communication between the grid and the consumer. In these legacy systems the consumers are passive entities whose operation can not be leveraged by the grid for supportive functions. In a smart grid however, information is shared bidirectionally which enables all the participants of energy trade to adjust their generation/consumption actively in order to ensure stable operation or to improve their welfare. The electrical network used in this thesis is assumed to be a smart distribution system with the following capabilities.

- The ability to offer information to prosumers (Selling price, Buying price, Operational/Transactional information).
- The ability to obtain information from prosumers (PV generation, ESS operation, Consumption).

- Self-awareness of the physical state of the distribution network (bus voltages, bus angles).
- Possessing a central computing system to execute the multi-layer P2P energy trading framework.

The traditional power consumers are only able to consume a fixed amount of power with no energy resources of their own; these are referred to in this study as 'legacy consumers'. The *prosumer*, in this thesis possesses a number of features that differentiate them from the legacy consumers, which are listed as follows [24].

- The ability to locally generate power through RES (PV, wind, hydro) and/or the ability to store energy for later use through ESS.
- The ability to vary their consumption within a defined range based on their flexibility.
- The ability to inject power into the grid for selling and to conduct financial transactions with other prosumers based on P2P energy exchanges..
- To offer information to the grid (PV generation, ESS operation, consumption).
- To obtain information from the grid (selling price, buying price, operational/transactional information).

As discussed in the introduction of this thesis, the P2P energy market is part of an emerging concept called Transactive Energy which is enabled by new smart grid technologies. The literature on P2P energy markets has proposed numerous strategies and approaches for optimal P2P energy trade. Some of these approaches have been discussed in the literature review, and are referred to in this thesis, as transactive energy strategies.

2.2 Utility Function of Prosumers

An important factor to consider when modeling prosumer behavior in a smart grid, is their satisfaction with the amount of power they are consuming. The 'satisfaction' or 'utility' that a prosumer gets by consuming a certain amount of electricity plays an important role in the decisions it will make in an optimization problem. Several functions have been used in the literature for the quantification of this utility; One of the commonly used functions is expressed as follows.

$$u_{i,t}(x_{i,t}) = \alpha_{i,t}x_{i,t} - \frac{\beta_i}{2}x_{i,t}^2 \tag{2.1}$$

where $x_{i,t}$ is the amount of power the prosumer i is consuming at time t and $u_{i,t}(x_{i,t})$ is the numerical value for the satisfaction obtained. The parameters $\alpha_{i,t}$ and β_i depend on the nature and size of the prosumer. Note that the $\alpha_{i,t}$ parameter varies with time for a prosumer i but the β_i parameter stays fixed over time. To understand their significance, one can consider two prosumers; Prosumer A is an extremely large house consuming 20 kW to keep the house heated at 22° C, and Prosumer B is a small house consuming 5 kW to maintain the same internal temperature. It is very likely that both the prosumers are getting the same level of satisfaction. Similarly at a different time it is possible that neither houses have a heating load, but are consuming the same amount of power and have the same utility. Hence these parameters need to be properly tuned to ensure that no unfair preference is given to a particular prosumer in the optimization process. Some of the following postulates have to be true for this function [25].

- The utility should be zero when there is no consumption i.e. $u(0) = 0$
- The value of the function should be non-decreasing i.e. $\frac{du}{dx} \geq 0$
- The marginal utility should be non-increasing i.e. $\frac{d^2u}{dx^2} \leq 0$

From the second and third postulate the structure of the utility function and its characteristics are evident. Since the function is non-decreasing, the inverted parabola shape is only used until its peak, after which point there is no increase in utility with increase in consumption.

2.3 Power Flow Equations for a Distribution System with Active Prosumers

If the specification and structure of the physical electrical network is known, one can evaluate the various parameters of electrical operation based on the power injections. This can be achieved by solving a set of power flow equations which require the following parameters to be formulated:

$$\mathbf{Y} = \begin{pmatrix} Y_{1,1} & Y_{1,2} & \cdots & Y_{1,bj} \\ Y_{2,1} & Y_{2,2} & \cdots & Y_{2,bj} \\ \vdots & \vdots & \ddots & \vdots \\ Y_{bi,1} & Y_{bi,2} & \cdots & Y_{bi,bj} \end{pmatrix} \tag{2.2}$$

$$\boldsymbol{\phi} = \begin{pmatrix} \phi_{1,1} & \phi_{1,2} & \cdots & \phi_{1,bj} \\ \phi_{2,1} & \phi_{2,2} & \cdots & \phi_{2,bj} \\ \vdots & \vdots & \ddots & \vdots \\ \phi_{bi,1} & \phi_{bi,2} & \cdots & \phi_{bi,bj} \end{pmatrix} \tag{2.3}$$

Where $\mathbf{Y}$ and $\boldsymbol{\phi}$ are the magnitude and phase matrices for the complex network admittance. The Power flow equations used to evaluate the system status are given as follows [26].

$$P_{bi}^{inj} = \sum_{bj \in \mathcal{B}} V_{bi} V_{bj} Y_{bi,bj} \cos\left(\phi_{bi,bj} + \theta_{bj} - \theta_{bi}\right) \qquad \forall bi \in \mathcal{B} \tag{2.4}$$

$$Q_{bi}^{inj} = -\sum_{bj \in \mathcal{B}} V_{bi} V_{bj,t} Y_{bi,bj} \sin\left(\phi_{bi,bj} + \theta_{bj,t} - \theta_{bi,t}\right) \qquad \forall bi \in \mathcal{B} \tag{2.5}$$

Where P_{bi}^{inj} and Q_{bi}^{inj} are the real and reactive power injections at bus bi, respectively. Since the prosumers are physically connected at the buses in the electrical network they can vary these injected powers by adjusting their own power exchange with the grid. This variability due to prosumer operation can be the result of either P2P energy trade or other grid supportive operations. It is important to note that this variability of power injection effectively renders the formulation as an Optimal Power Flow (OPF) problem. The active and reactive powers injected into a bus bi consists of two components, shown as follows :

$$P_{bi}^{inj} = P_{bi}^{fixed} + P_{bi}^{variable} \qquad \forall bi \in \mathcal{B} \tag{2.6}$$

$$Q_{bi}^{inj} = Q_{bi}^{fixed} + Q_{bi}^{variable} \qquad \forall bi \in \mathcal{B} \tag{2.7}$$

Where the P_{bi}^{fixed} and Q_{bi}^{fixed} components are fixed values which represent the traditional consumers and loads which are not actively participating in any smart grid tasks. $P_{bi}^{variable}$

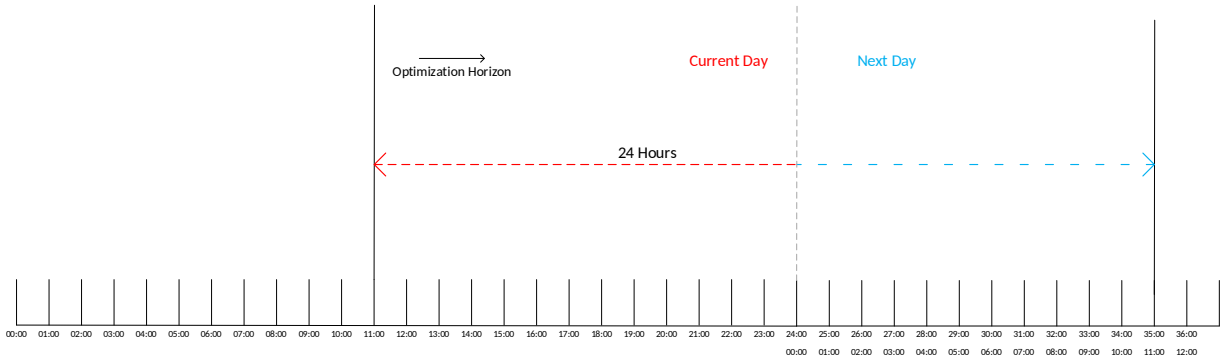

Figure 2.1: Time horizon unwrapped view

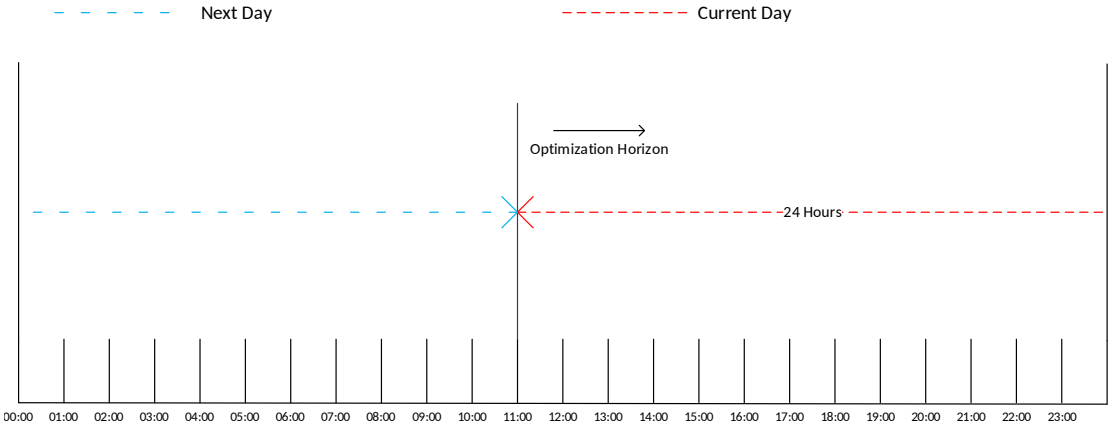

Figure 2.2: Time horizon wrapped view

and $Q_{bi}^{variable}$ on the other hand depend on the prosumers connected at the bi bus. These components are positive when power is injected into the grid from an energy resource, and is negative when it is being extracted from the grid as is the case when power is consumed by prosumers. Thus, in a system with active prosumers, these variable power injections can be set equal to the total power exchanged by the prosumers through the system.

2.4 Model Predictive Control

MPC in the context of power systems refers to the algorithmic approach of repetitive optimization at each interval for which a decision is to be made. This requirement arises due to uncertainties in the future status of the power system for which a forecast is generated.

The accuracy of these forecasts worsens when the forecasting horizon is distant and improves as it grows closer. Hence successive optimizations can be carried out at each interval with a better forecast than the previous. The optimal decisions generated through such successive optimization are only applied for that specific interval. A time period needs to be selected over which the system objective is to be optimized.

A 24 hour receding horizon is selected in this thesis considering the repetitive nature of daily operations. To understand this approach note the optimization horizon in Fig.2.1 for an optimization that is being executed at Hour 11:00 with length extending to Hour 35:00, which is essentially Hour 11:00 for the next day. Hence this portion of the horizon can be placed on the same 24 hour interval as shown in Fig.2.2. The practical benefit of this MPC approach is that the objective developed for a 24 hour operation does not need to be reformulated, and simply executing the optimization model again after modifying the data parameters, is sufficient.

The focus of MPC in power systems so far has been restricted to the inclusion of known uncertainties where the forecasts of parameters gradually become more and more accurate as they get closer. This is an incomplete picture however, since there can be uncertainties in the system which are highly unpredictable and unforecastable. These uncertainties only make their effect known in the interval they occur and the MPC technique should be able to actively respond to them as well.

2.5 Summary

The idea of a smart grid and prosumers in relation to each other were discussed in this chapter along with some of their salient features. Then the utility function used in this thesis is explained along with the reasoning behind how the numerical value of utility relates to prosumer satisfaction; the postulates of a viable utility function are subsequently discussed. Next, the integration of power flow equations into a system with active prosumers is discussed. Finally the MPC approach used in this study is explained.

Chapter 3

A Multi-Layer Framework for Peer-to-Peer (P2P) Energy Trade Considering Dynamic Operation of Prosumers

It is evident that prosumers need to be granted greater operational freedom in terms of their electricity consumption and that a generalized physical layer is needed to ensure that any P2P energy trades are compliant with the physical network constraints. To address these issues, a novel framework is proposed in this chapter for P2P energy trade that merges the physical and virtual layers into a multilayer framework that is flexible and can be implemented with any transactive energy strategy.

3.1 Proposed Multi-Layer Framework for P2P Energy Markets

It is assumed that each prosumer is equipped with an intelligent power controller which is directed by a central computing system that executes the framework developed in this chapter to determine the optimal prosumer decisions and energy transactions.

3.1.1 P2P Energy Market Objectives

The proposed multi-layer framework can be directed to optimize certain system parameters guided by objective functions. These objectives are discussed as follows.

Prosumer Welfare Maximization

This objective represents prosumer satisfaction, which is modeled using a utility function $u_{i,t}(x_{i,t})$. Similar functions have been used in other works [11], [7].

$$u_{i,t}(x_{i,t}) = \alpha_{i,t}x_{i,t} - \frac{\beta_i}{2}x_{i,t}^2 \qquad \forall i \in \mathcal{N}\ ;\ \forall t \in \mathcal{T} \tag{3.1}$$

where $\alpha_{i,t}$ and β_i are fixed parameters denoting prosumer satisfaction with their consumption. These are determined by normalizing the peak utility value that a prosumer can obtain from power consumption, as follows.

$$u_{i,t}(D_{i,t}^{\max}) \approx \text{constant} \qquad \forall i \in \mathcal{N}\ ;\ \forall t \in \mathcal{T} \tag{3.2}$$

The value of this utility cannot be directly obtained from (3.2) due to the nature of the function. The peak occurs at the point where $\frac{du}{dx} = 0$ and hence $x_{i,t} = \frac{\alpha_{i,t}}{\beta_i}$ which when plugged back into the utility function (3.1) yields a peak value of $\frac{\alpha_{i,t}^2}{2\beta_i}$. This peak value should occur when the prosumer is consuming power at the upper limit, i.e. $x = D_{i,t}^{\max} = \frac{\alpha_{i,t}}{\beta_i}$. Since the peak satisfaction for all prosumers at each hour is set as constant, i.e. $\frac{\alpha_{i,t}^2}{2\beta_i} = \text{constant}$, and b_i parameter is also constant for each prosumer, it is noted that algebraically the value $\frac{\alpha_{i,t}}{\beta_i}$ for the same prosumer for differing values of $D_{i,t}^{\max}$ cannot be varied. Hence the following approach is utilized in this study to obtain these parameters.

In order to obtain the best approximations for these parameters, constant values are assigned for the peak utility of each prosumer. Note that this peak utility may be considered to vary from prosumer to prosumer, and even over time, for each prosumer depending on the approach. In this study since most of the prosumers are nearly of the same size, their peak utility is assumed to vary with time; as follows,

$$u_{i,t}(D_{i,t}^{\max}) = k_i D_{i,t}^{\max} \pi_{avg}^{G2P} \qquad \forall i \in \mathcal{N}\ ;\ \forall t \in \mathcal{T} \tag{3.3}$$

where k_i is a parameter used to set the maximum satisfaction value of a prosumer. This k_i parameter can be varied to change the importance of certain prosumers or to ensure each prosumer has the same numerical utility regardless of maximum consumption. The peak should occur at the point where $D_{i,t}^{\max} = \frac{\alpha_{i,t}}{\beta_i}$ and hence the following objective function is formulated by setting the parameters $\alpha_{i,t}$ and b_i as variables.

$$\text{Min } J = \sum_{i \in \mathcal{N}} \sum_{t \in \mathcal{T}} ((u_{i,t}(D_{i,t}^{\max}) - k_i D_{i,t}^{\max} \pi_{avg}^{G2P})^2 + (\alpha_{i,t} - \beta_i D_{i,t}^{\max})^2) \tag{3.4}$$

Minimizing the above objective yields values for these prosumer parameters. The total prosumer welfare $W_{i,t}$ is then formulated by considering the cost of power exchange in addition to the utility function, given as follows;

$$\begin{aligned} W_{i,t} = u_{i,t}(x_{i,t}) + \pi_t^{P2G} P_{i,t}^{P2G} - \pi_t^{G2P} P_{i,t}^{G2P} \\ + \pi_t^{P2P} \sum_{j \in \mathcal{N}} x_{i,j,t}^{P2P} - \pi_t^{P2P} \sum_{j \in \mathcal{N}} x_{j,i,t}^{P2P} \\ \forall i \in \mathcal{N} \; ; \; \forall t \in \mathcal{T} \end{aligned} \tag{3.5}$$

where the second and fourth terms represent the revenue earned by the prosumer when selling power to the grid or in the P2P market, respectively; the third and fifth terms are the cost of purchasing power from grid and P2P market, respectively. Note that, depending on the prosumer's buyer or seller status at time t, either the revenue or the cost terms shall be non-zero as will be discussed later. The total welfare function is then used as the system objective for maximization, as follows.

$$\text{Max } Welfare = \sum_{i \in \mathcal{N}} \sum_{t \in \mathcal{T}} W_{i,t} \tag{3.6}$$

In (3.6), the summation of welfares over all time intervals for all prosumers shall cancel out the P2P revenues and costs (fourth and fifth terms) since the revenue of a seller is equal to the cost incurred by a buyer.

Prosumer Cost Minimization

This objective seeks to minimize the total cost of power purchased by prosumers from the grid, which essentially translates to limiting the prosumers' reliance on the grid and

encourages them to operate independently. [15]

$$\text{Min } Cost = \sum_{i \in \mathcal{N}} \sum_{t \in \mathcal{T}} \pi_t^{G2P} P_{i,t}^{G2P} \tag{3.7}$$

System Loss Minimization

This objective seeks to improve grid operational efficiency by minimizing feeder losses, and analyzes the extent prosumers can contribute to improve grid operations.

$$\text{Min } Losses = \frac{1}{2} \sum_{t \in \mathcal{T}} \sum_{bi \in \mathcal{B}} \sum_{bj \in \mathcal{B}} Y_{bi,bj} \cos \phi_{bi,bj} \left[V_{bi,t}^2 + V_{bj,t}^2 - 2 V_{bi,t} V_{bj,t} \cos \left(\theta_{bj,t} - \theta_{bi,t} \right) \right] \tag{3.8}$$

3.1.2 Virtual Layer

Prosumer ESS Model

A commonly used ESS operational model is adopted, with the novel addition of a circular boundary condition, as shown below.

$$E_{i,t} = E_{i,t-1} + (P_{i,t-1}^{Ch} \eta_i^{Ch} - P_{i,t-1}^{Dch} / \eta_i^{Dch}) \Delta t \qquad \forall i \in \mathcal{N} \; ; \; \forall t \in \{2, 3, 4, ..., T\} \tag{3.9}$$

$$E_{i,1} = E_{i,T} + (P_{i,T}^{Ch} \eta_i^{Ch} - P_{i,T}^{Dch} / \eta_i^{Dch}) \Delta t \qquad \forall i \in \mathcal{N} \tag{3.10}$$

Note that (3.9) is not applicable to the first time interval, and has been linked to the boundary interval T using (3.10). By removing a strict boundary for start and end intervals, the P2P system can achieve better prosumer operation, as will be discussed later in Section III.

The maximum charging and discharging power limits are defined as follows:

$$0 \leq P_{i,t}^{Ch} \leq b_{i,t}^{Ch} P_i^{Ch_{\max}} \qquad \forall i \in \mathcal{N} \; ; \; \forall t \in \mathcal{T} \tag{3.11}$$

$$0 \leq P_{i,t}^{Dch} \leq b_{i,t}^{Dch} P_i^{Dch_{\max}} \qquad \forall i \in \mathcal{N}\ ;\ \forall t \in \mathcal{T} \tag{3.12}$$

where $b_{i,t}^{Ch}$ and $b_{i,t}^{Dch}$ are binary variables that indicate the charging and discharging status of the ESS, respectively. The mutual exclusivity of the binary status variables is given as follows.

$$b_{i,t}^{Ch} + b_{i,t}^{Dch} \leq 1 \qquad \forall i \in \mathcal{N}\ ;\ \forall t \in \mathcal{T} \tag{3.13}$$

Prosumer Power Consumption

The power consumption of a prosumer is flexible within a range, as given below.

$$D_{i,t}^{\min} \leq x_{i,t} \leq D_{i,t}^{\max} \qquad \forall i \in \mathcal{N}\ ;\ \forall t \in \mathcal{T} \tag{3.14}$$

Dynamic Prosumer Classification

The status of a prosumer as a seller or a buyer depends on its surplus power availability. The prosumer, being flexible, can adjust its consumption as shown in (3.14), and adjust the ESS charging/discharging power as shown in (3.11), (3.12). By leveraging the above adjustments, under the effect of internal (PV generation) and external (TOU price, Feed-in-Tariff) parameters, the prosumer can dynamically change its status, as shown in Fig.3.1. These dynamics are described through the following equations.

$$P_{i,t}^{PV} \leq x_{i,t} + P_{i,t}^{Ch} - P_{i,t}^{Dch} + \mathbb{M} s_{i,t} \qquad \forall i \in \mathcal{N}\ ;\ \forall t \in \mathcal{T} \tag{3.15}$$

$$x_{i,t} + P_{i,t}^{Ch} - P_{i,t}^{Dch} \leq P_{i,t}^{PV} + \mathbb{M}(1 - s_{i,t}) \qquad \forall i \in \mathcal{N}\ ;\ \forall t \in \mathcal{T} \tag{3.16}$$

If the status variable $s_{i,t}$ is Boolean True, it indicates the prosumer's status as a seller, otherwise the prosumer is a buyer.

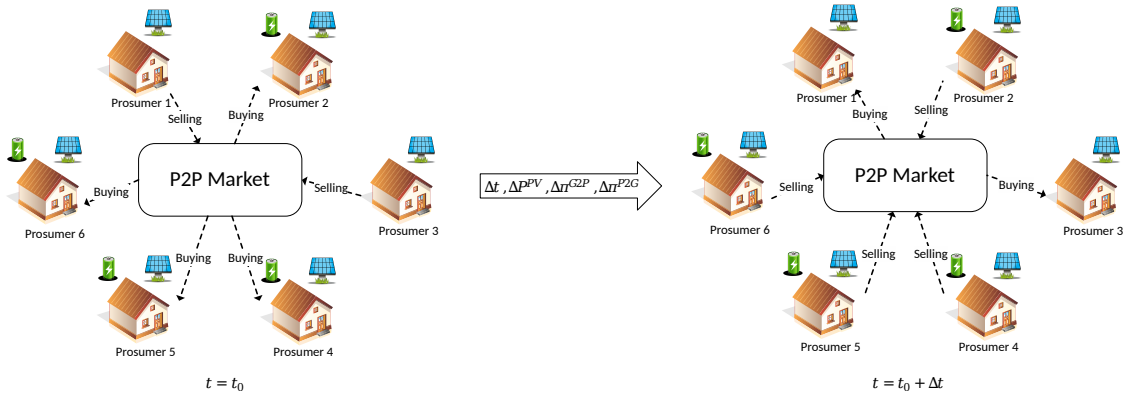

Figure 3.1: P2P energy market showing prosumers behaving dynamically with change in time, PV generation, TOU price, Feed-in-Tariff

Prosumer Power Balance and Exchange

Based on prosumer decisions, the surplus power is sold to either the grid or in the P2P market. Similarly if there is a power deficit, the required power is purchased from the grid or the P2P market. The following balance equations describe this exchange.

$$P_{i,t}^{PV} + P_{i,t}^{Dch} - P_{i,t}^{Ch} - x_{i,t} = \sum_{j \in \mathcal{N}} x_{i,j,t}^{P2P} + P_{i,t}^{P2G} - \sum_{j \in \mathcal{N}} x_{j,i,t}^{P2P} - P_{i,t}^{G2P}$$

$$\forall i \in \mathcal{N} \; ; \; \forall t \in \mathcal{T} \quad (3.17)$$

where $P_{i,t}^{G2P}$, $P_{i,t}^{P2G}$ and $x_{i,j,t}^{P2P}$ are positive variables and the power sold or purchased by a prosumer depends on its dynamic status at time t.

$$\sum_{j \in \mathcal{N}} x_{i,j,t}^{P2P} + P_{i,t}^{P2G} \leq \mathbb{M} s_{i,t}$$

$$\forall i \in \mathcal{N} \; ; \; \forall t \in \mathcal{T} \quad (3.18)$$

$$\sum_{j \in \mathcal{N}} x_{j,i,t}^{P2P} + P_{i,t}^{G2P} \leq \mathbb{M}(1 - s_{i,t})$$

$$\forall i \in \mathcal{N} \; ; \; \forall t \in \mathcal{T} \quad (3.19)$$

$$x_{i,i,t}^{P2P} = 0 \qquad \forall i \in \mathcal{N}\ ;\ \forall t \in \mathcal{T} \quad (3.20)$$

The inequality (3.18) ensures that a prosumer can only sell power when it has the status of a seller. Similarly (3.19) ensures that power purchase is only possible when a prosumer has the status of a buyer. Finally (3.20) ensures that a prosumer cannot sell power to itself.

P2P Market Pricing

A Mid-Market Rate (MMR) strategy is used in this work to set a price of power in the P2P market. This strategy has been used in other literature aswell [8], [27]. The P2P market price is computed as follows.

$$\pi_t^{P2P} = \frac{\pi_t^{P2G} + \pi_t^{G2P}}{2} \qquad \forall t \in \mathcal{T} \quad (3.21)$$

3.1.3 Physical Layer

Prosumer Physical Placement

The physical placement of a prosumer in the electric network is taken into account in this layer using an Incidence Matrix $\mathbf{C^{LOC}}$ defined on $\mathcal{N} \times \mathcal{B}$. The elements are defined as follows.

$$C_{i,bi}^{LOC} = \begin{cases} 1 & \text{if prosumer } i \text{ is connected at bus } bi \\ 0 & \text{otherwise} \end{cases} \quad (3.22)$$

This is a predetermined parameter since a prosumer's location is fixed in the grid. In this approach care must be taken to ensure that a prosumer is not placed on multiple buses simultaneously. Multiple prosumers can however be connected at the same bus.

Prosumer Grid Exchange

Power exchanged by a prosumer with the grid, $P_{i,t}^{inj}$, has to satisfy the following balance relation.

$$P_{i,t}^{inj} = P_{i,t}^{PV} + P_{i,t}^{Dch} - P_{i,t}^{Ch} - x_{i,t} \qquad \forall i \in \mathcal{N}\ ;\ \forall t \in \mathcal{T} \quad (3.23)$$

In (3.23), $P_{i,t}^{inj}$ is positive when the prosumer has the status of a seller and is selling power to the grid or in the P2P market, and negative when it is buying power.

Power Flow Equations for a System Hosting a Dynamic P2P Market

To capture the impacts of P2P energy transactions on the physical electrical network, $P_{i,t}^{inj}$ is used in conjunction with $\mathbf{C^{LOC}}$ to evaluate the power flows, as given below.

$$\left(\sum_{\forall i \in \mathcal{N}} C_{i,bi}^{LOC} P_{i,t}^{inj} - P_{bi,t}^{load}\right) / S_{base} = \sum_{bj \in \mathcal{B}} V_{bi,t} V_{bj,t} Y_{bi,bj} \cos\left(\phi_{bi,bj} + \theta_{bj,t} - \theta_{bi,t}\right) \quad \forall bi \in \mathcal{B}\ ;\ \forall t \in \mathcal{T} \quad (3.24)$$

$$\left(\sum_{\forall i \in \mathcal{N}} C_{i,bi}^{LOC} Q_{i,t}^{inj} - Q_{bi,t}^{load}\right) / S_{base} = -\sum_{bj \in \mathcal{B}} V_{bi,t} V_{bj,t} Y_{bi,bj} \sin\left(\phi_{bi,bj} + \theta_{bj,t} - \theta_{bi,t}\right) \quad \forall bi \in \mathcal{B}\ ;\ \forall t \in \mathcal{T} \quad (3.25)$$

$$0.9 \leq V_{bi,t} \leq 1.1 \quad \forall bi \in \mathcal{B}\ ;\ \forall t \in \mathcal{T} \quad (3.26)$$

where P_{bi}^{load} and Q_{bi}^{load} are non-participating base loads connected to a bus, and S_{base} is assumed to be 10 MVA. The left hand side of (3.24) and (3.25) contains variables having units of kW and kVAR respectively, which are converted to per-unit. In this study the prosumer is assumed to be incapable of generating reactive power and has a fixed reactive power demand profile. Hence the injected reactive power $Q_{i,t}^{inj}$ will always be negative.

3.2 Implementation and Results

The 33 bus distribution feeder [28] is used for the present studies, as shown in Fig.3.2, which also indicates the random physical placement of 12 ($N = 12$) prosumers, considered in this work. Ideal prosumer placement is not within the scope of this study. All prosumers have PV generation while prosumers 1 to 5 are also equipped with an ESS of 30 kW/200 kWh capacity, each, and efficiency of 90%. Simulations are carried out over a 24-hour period ($T = 24$), with 1 hour time intervals, $\Delta t = 1$.

The prosumer load and PV power profiles have been generated using an open source, Python-based load profile generator [29], considering the prosumers to be large entities which realistically can be residential buildings or housing clusters. A separate profile is generated for each prosumer in the set $\mathcal{N} = \{1, 2, 3, ..., N\}$, over a set of time-intervals $\mathcal{T} = \{1, 2, 3, ..., T\}$, given as follows:

$$\mathbf{P_i^{PV}} = \{P_{i,1}^{PV}, P_{i,2}^{PV}, P_{i,3}^{PV}, ..., P_{i,T}^{PV}\} \quad \forall i \in \mathcal{N} \quad (3.27)$$

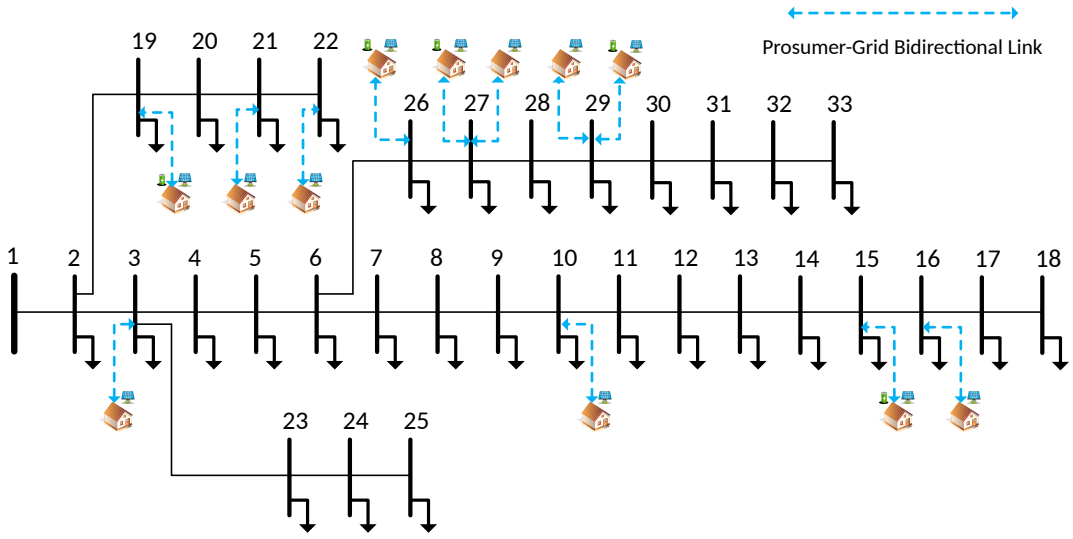

Figure 3.2: 33 Bus system hosting 12 prosumers

$$\mathbf{D_i^{max}} = \{D_{i,1}^{\max}, D_{i,2}^{\max}, D_{i,3}^{\max}, ..., D_{i,T}^{\max}\} \quad \forall i \in \mathcal{N} \tag{3.28}$$

$$\mathbf{D_i^{min}} = \{D_{i,1}^{\min}, D_{i,2}^{\min}, D_{i,3}^{\min}, ..., D_{i,T}^{\min}\} \quad \forall i \in \mathcal{N} \tag{3.29}$$

The given load data of the 33-bus system was transformed to 24-load profile at each bus using the same Python based load profile generator. The total load at a bus at any hour, comprises the non-participating, generated bus loads which are fixed ($P_{bi,t}^{load}, Q_{bi,t}^{load}$) and the prosumer power exchanges with the grid ($P_{i,t}^{inj}, Q_{i,t}^{inj}$), as given in (3.23), (3.24) and (3.25). The non-participating bus loads are shown in Fig.3.3.

The "base" real and reactive power demand of prosumers is shown in Fig.3.4, The real power demand will vary because of prosumer's flexibility, as given in (3.14); $D_{i,t}^{\min}$ and $D_{i,t}^{\max}$ are obtained by assuming a 25% flexibility from the base demand. The PV generation from each prosumer is also shown in Fig.3.4, which is non-zero during the time interval from 6:00 to 21:00 hours. Prosumer behaviors are significantly influenced by the tariff rates set by the utility for power exchanges. The price (π_t^{G2P}) when buying from the grid is considered to be a Time of Use (TOU) tariff that consists of three levels; 0.101 \$/kWh at off-peak (1:00 - 6:00, 19:00 - 24:00), 0.144 \$/kWh at the mid-peak (7:00 - 10:00, 17:00 - 18:00) and 0.208 \$/kWh during the on-peak hours (11:00 - 16:00). For selling power to the grid (π^{P2G}), a Feed-in-Tariff rate of 0.05 \$/kWh is assumed.

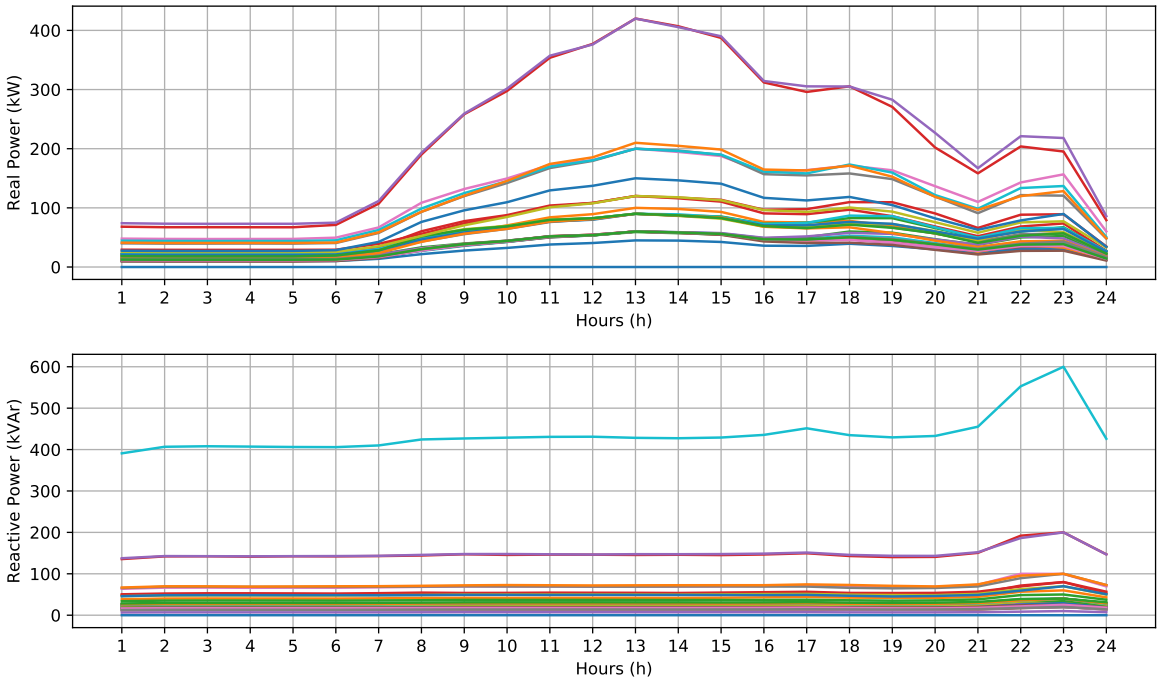

Figure 3.3: Non-participating real and reactive power profiles for 33 buses in the system (legend not attached because profile pattern is visible without specifying bus locations)

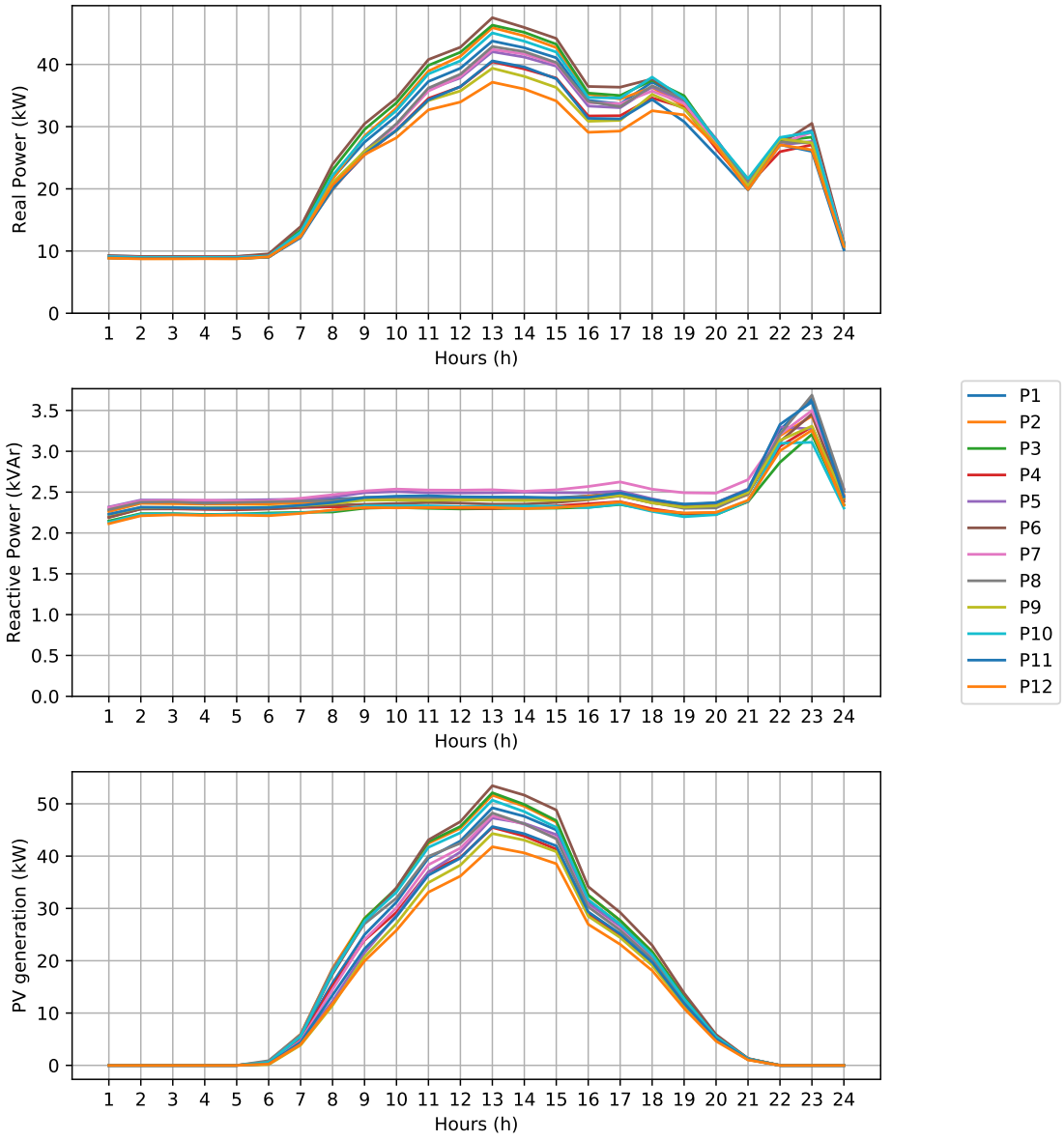

Figure 3.4: Prosumer "base" consumption and PV generation

3.2.1 Case-0: Base Case, Legacy Consumer

The base case for comparison assumes that prosumers have no P2P capability, DERs, or consumption flexibility. The Base Case renders them effectively as a *legacy consumer* wherein their consumption is denoted by a fixed, generated load profile ($x_{i,t}$) shown in Fig.3.4.

3.2.2 Case-1: Prosumer Welfare Maximization

In this case, the collective behavior of the prosumers is governed by the cost of buying power from the grid, *i.e.*, the TOU tariff. Notice that Fig.3.5 shows that prosumers charge their ESS early in the day. Since no PV generation is available at these hours, the power for self-consumption and charging the ESS is purchased from the grid at low TOU price and this behavior continues until 7:00, after which the TOU price increases.

Figure 3.6 shows that the power sold by prosumers in the P2P market is high at certain hours. These high P2P exchanges occur when the TOU tariff is at mid-peak and the prosumers' PV generation are insufficient to meet their own demand. This supply deficit is met by prosumers with ESS who discharge to participate in the P2P market because of the moderately high TOU tariff at these hours. This strategy demonstrates dynamic prosumer behaviour which enables them to adjust their consumption and to act as sellers when it is beneficial to do so. This operating strategy continues until the PV power increases and meets the prosumer's self-demand (at hours 12:00-15:00) when the roles are flipped. The prosumers with ESS now act as buyers to purchase the surplus energy from prosumers without ESS and store until the PV generation again falls below prosumer's self-demand (at 16:00 - 18:00), at which point the batteries are discharged to sell power in the P2P market, as shown in Fig.3.5 and Fig.3.6. Finally the ESS are again charged by purchasing power from the grid at off-peak hours, as per the circular boundary constraints defined in (3.10).

The power exchanges among prosumers over the 24-hour period are depicted as a heatmap in Fig.3.7, which shows that prosumers with ESS (P1 - P5) primarily behave as sellers while the non-ESS prosumers primarily act as buyers; the behavior pattern may be inferred by comparing with Fig.3.5 and Fig.3.6, as well.

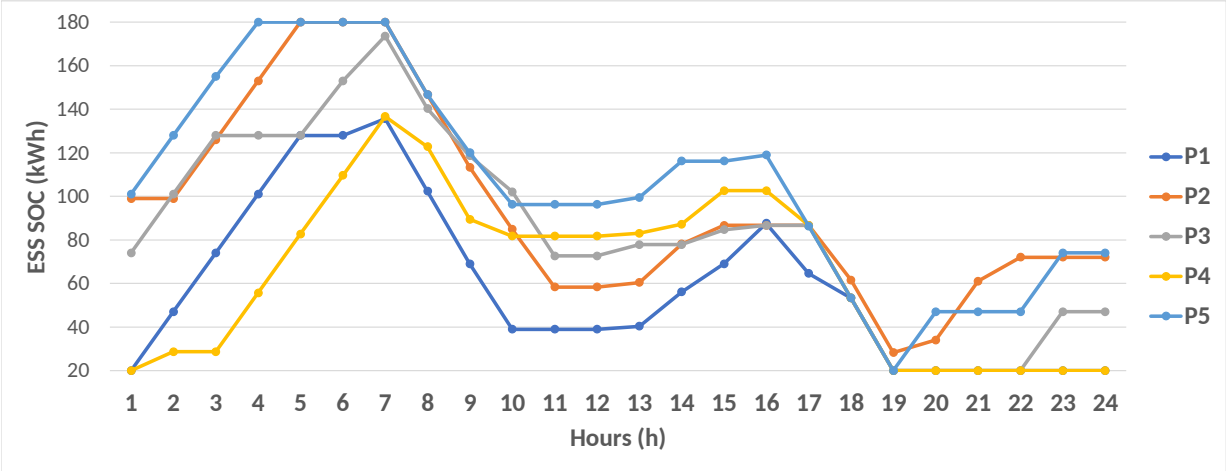

Figure 3.5: Case 1: SOC of prosumer ESS

3.2.3 Case-2: Prosumer Cost Minimization

In this case the P2P market exchanges take place for most of the day to minimize the prosumers' cost of purchasing power from the grid (Fig. 3.9 and Fig.3.8). It is noted that during the early hours before PV generation is available (1:00 - 8:00) batteries are discharged by prosumers with ESS to meet the required demand and participate in P2P market. More P2P exchanges occur during the peak PV generation hours (12:00 - 15:00) because of power surplus of prosumers with their reduced consumption as flexibility allows. This surplus PV power is purchased by prosumers with ESS to charge their batteries, as can be noted from the SOC plots in Fig.3.8, which are again discharged as PV generation falls (16:00 - 24:00), to meet their self-demand and for selling in the P2P market. Any power purchased from the grid is limited to hours when the TOU tariff is lowest. The heatmap for this case (Fig.3.10) shows relatively higher levels of activity in the P2P market. In contrast to Case-1, the prosumers with ESS primarily act as buyers purchasing surplus power from prosumers without ESS and minimize their purchase from the grid even when TOU tarrif is low.

This operation indicates how critical it is to allow prosumers to behave dynamically since a static approach would severely limit the strategies a prosumer could deploy to minimize costs.

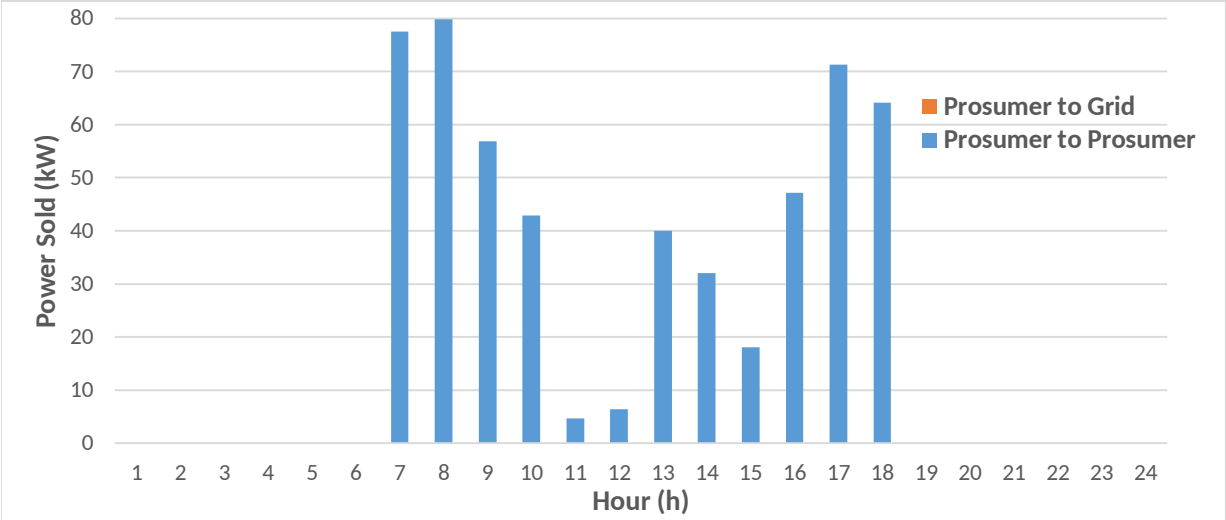

Figure 3.6: Case 1: Power sold by prosumer

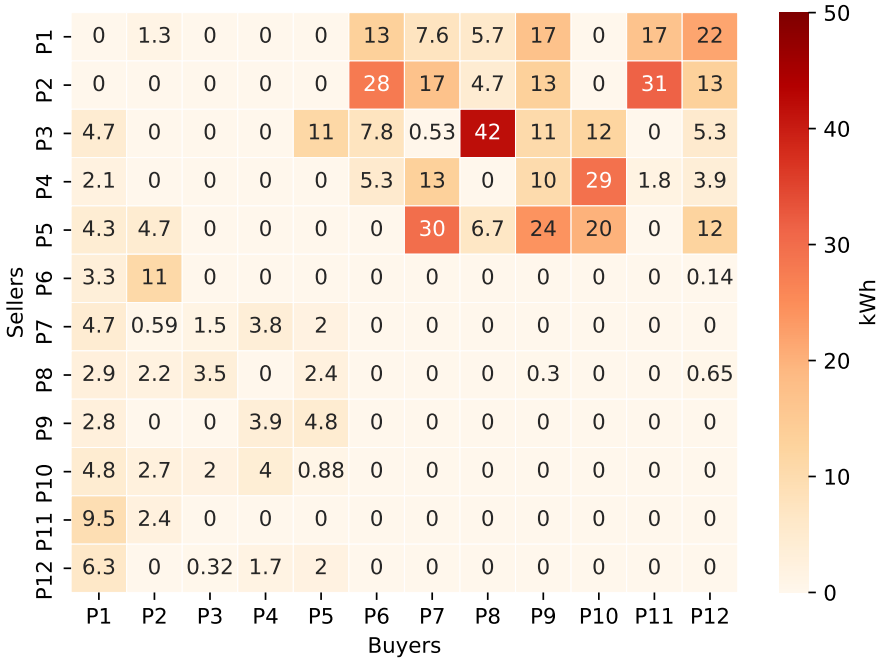

Figure 3.7: Case 1: Heatmap of P2P energy exchange aggregated over 24 hours

3.2.4 Case-3: System Loss Minimization

In this case, the prosumers receive dispatch instructions from the utility, which are based on the loss minimization objective. The load in the system varies over the day as seen in Fig.3.3 which shows peak consumption between 11:00 and 16:00. The operating strategy directs prosumers with ESS to purchase power from the grid for charging, during the off-peak TOU tariff hours, which is then discharged during the peak demand hours (Fig.3.11). Similarly, prosumers without ESS are directed to inject their surplus power into the grid. The contribution from all prosumers during peak hours is noted in Fig.3.12. A heatmap is not presented in this case since there is very little activity in the P2P market.

3.2.5 Case Comparison and Discussion

The physical status of the feeder hosting the prosumers can be determined from its bus voltages, line flows and losses. In this study, the peak load on the 33 bus system occurs at 13:00 hours (Fig.3.3) and the system voltages at this hour, for the various cases, are presented in Fig.3.14. As expected, Case-3 (Loss Minimization) presents the best voltage profile in the system, with the lowest voltage drop across the feeder buses. Note that the voltage profiles for Case-1 (Welfare Maximization) and Case-2 (Cost Minimization) are very similar at 13:00 hour because the prosumers' PV generation is sufficient to meet their demand and only the surplus power is traded in the P2P market where prosumers with ESS purchase this surplus to charge their batteries; the nature of trade is the same in both cases. Furthermore, the power sold by prosumers at 13:00 hours in Case-3 is much larger than in other cases, which effectively increases the net power injection into the grid, hence yielding a visibly improved system voltage profile.

A comparison of the system variables for various optimization objectives (i.e. Cases), aggregated over the 24-hour horizon, is presented in Table.3.1. In the Base Case, the prosumers are assumed to be normal power consumers without DERs or flexible consumption. In Case-1, prosumers are incentivized to consume more power, depending on the choice of the utility function (3.1) parameters. This is noted from the total prosumer consumption and welfare, which are higher than the other cases. The cost minimization objective (Case 2) indicates high P2P energy exchanges, which yield the lowest operating cost. For the loss minimization objective (Case 3), significant amount of power is injected into the grid at peak hours to minimize the power losses.

The financial benefits for prosumers with DERs, from the proposed multi-layered framework, as compared to legacy consumers (no consumption flexibility and no DERs) are

shown in Fig.3.13, depicting the total savings for prosumers in each case, over the 24-hour operating horizon. The savings in Case-1 are highest for every prosumer and can be attributed to their overall higher consumption as noted in Table. 3.1. Total prosumer consumption in Cases-2 and -3 are quite similar but the prosumer savings in Case-2 are higher, as noted from Fig.3.13, because of the different strategies used when minimizing total prosumer cost as against total system losses. The prosumers' hourly financial transactions further reflect the strategies employed by them for each of the cases in this study. The transactions for two prosumers, one with ESS and one without, are presented in Fig.3.15 and Fig.3.16 respectively, where a negative financial transaction denotes payments by prosumers for energy purchase, while positive denotes revenue acrued from energy sold. Note that prosumers with ESS show their preference to purchase surplus power from prosumers without ESS during peak generation hours (11:00 - 15:00) as discussed earlier.

Additional inferences regarding prosumer operation can be made from the P2P energy exchange heatmaps in Fig.3.7 and Fig.3.10, and the SOC plot of ESS in Fig.3.5, Fig.3.8 and Fig.3.11. Note that both the heatmaps show energy exchanges clustered in regions between prosumers who have ESS (P1-P5) with those that have none (P6-P12). Exchanges among prosumers without ESS are noted to be very small, in both cases. These outcomes arise due to the variance in ESS capability and uniformity of generation, respectively. Therefore, it can be inferred that in order to achieve high P2P participation, diversity in prosumer capabilities has a catalyzing effect. From the SOC plots of ESS, the benefit of enabling a circular boundary constraint (3.10) is readily apparent. For example, in Case-3, the ESS is fully charged before peak hours so as to fully discharge by the end of the day, in Case-1 the ESS is charged for energy trade with other prosumers when the TOU price increases and in Case-2, the ESS is discharged very early in the day for self-consumption to minimize reliance on the grid electricity. These strategies would not have been as effective if the SOC at the boundary of the simulation interval had been fixed to a certain value.

3.3 Summary

A comprehensive P2P energy trading framework was introduced in this chapter which was centered around a dynamically acting prosumer, whose flexibility could be leveraged to improve system operations and social welfare. A physical electrical network was also incorporated into this framework to ensure that all prosumer actions and market decisions would conform to the physical constraints of the network. The notable novel aspects of this framework are: the development of a dynamic prosumer operation model, which includes ESS storage with modified circular boundary constraints, and generalized physical layer

Table 3.1: System behavior under the various optimization objectives

System Variables \ Cases	Case-1	Case-2	Case-3	Case-0
Total Welfare ($)	5842	5138	5024	N/A
Total Power Loss (p.u.)	0.224	0.216	0.207	0.252
Total Prosumer Power Cost ($)	360	101	175	1104
Total Prosumer Savings ($)	861	762	654	N/A
Total Prosumer Consumption (kWh)	8059	5533	5369	7150
Total P2P Exchange (kWh)	541	921	57	N/A
Total Energy Sold to Grid (kWh)	0	0	1665	N/A

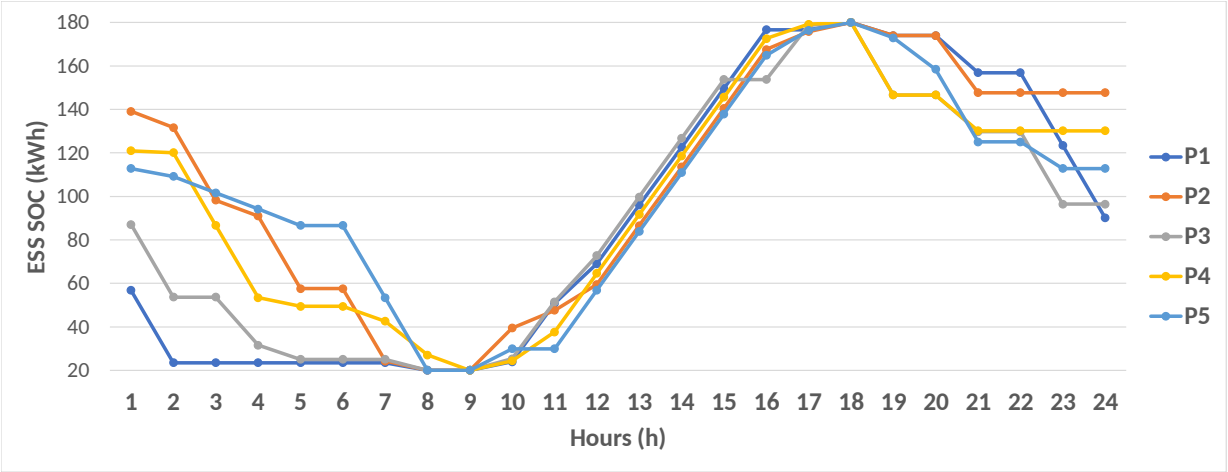

Figure 3.8: Case 2: SOC of Prosumer ESS

integration.

Several objectives were formulated to direct prosumer operations towards their own benefit and for the benefit of the grid. These objectives were then simulated on a 33-bus system and the prosumer responses were subsequently analyzed and discussed for each of the developed market objectives along with the numerical comparison of the various system parameters. The benefits of the novel components listed above were demonstrated when the prosumers were shown to adjust their operations to participate in the P2P market at times, which would have otherwise been restrictive in static P2P models. Furthermore, the possible participation of prosumers in grid support functions such as loss minimization, was also shown to be effective.

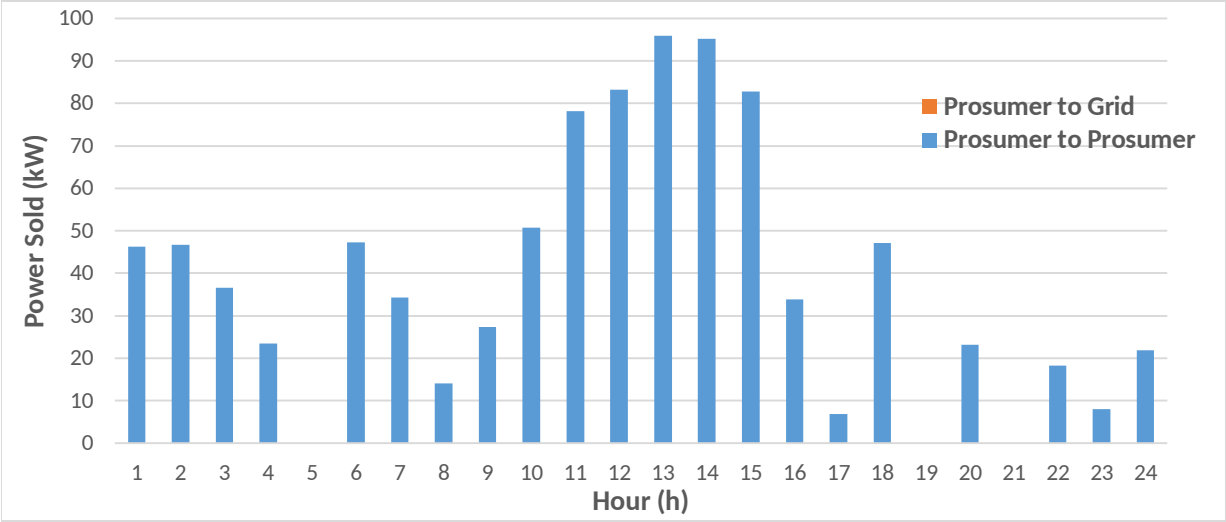

Figure 3.9: Case 2: Power sold by prosumers

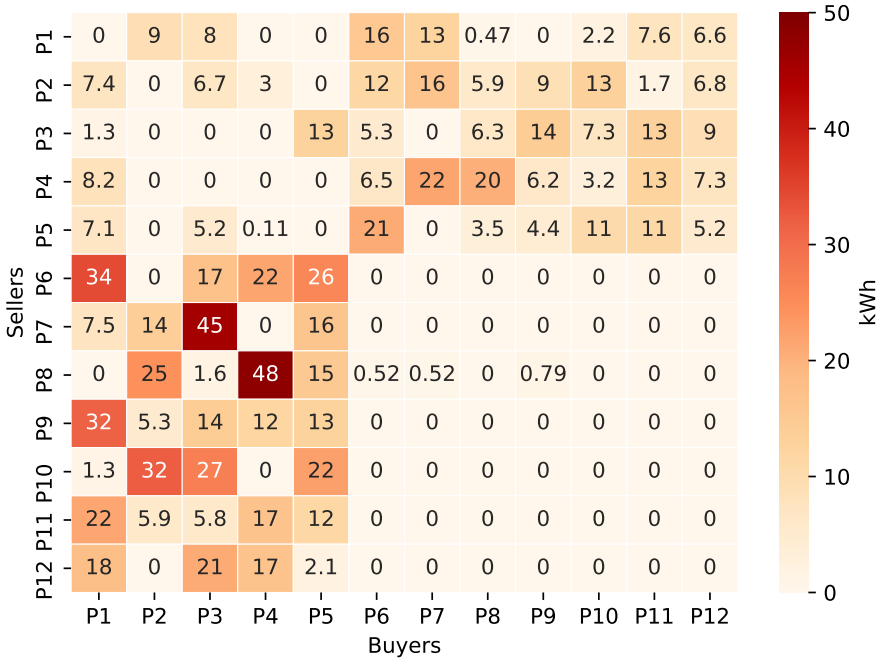

Figure 3.10: Case 2: Heatmap of P2P energy exchange aggregated over 24 hours

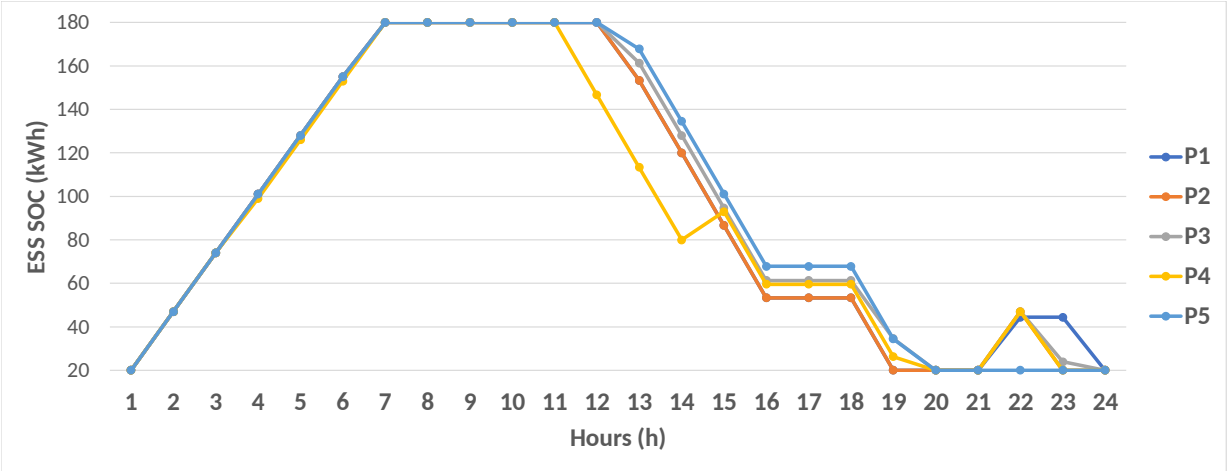

Figure 3.11: Case 3: SOC of Prosumer ESS

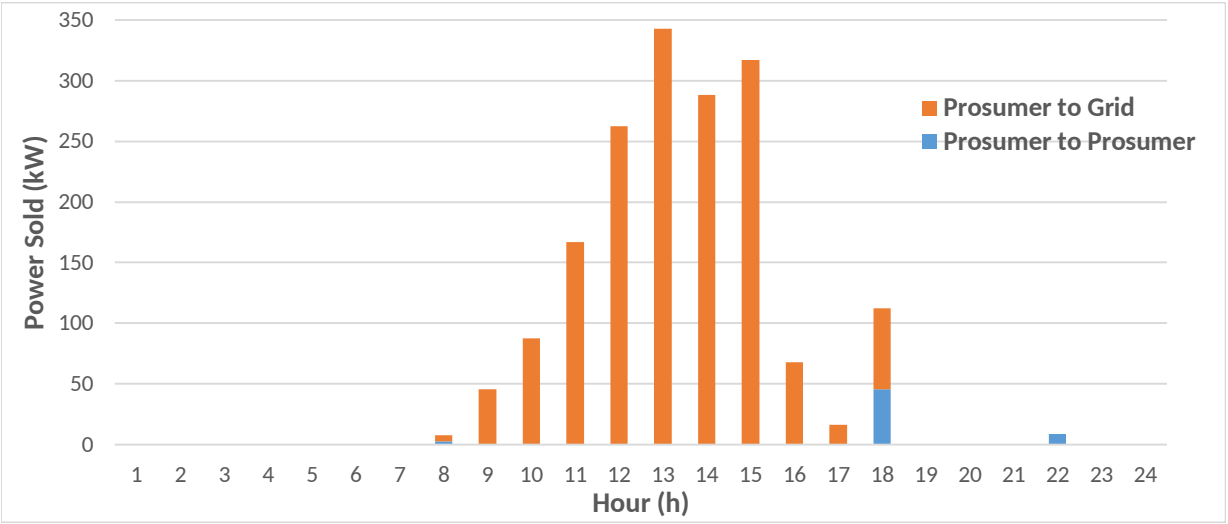

Figure 3.12: Case 3: Power sold by prosumers

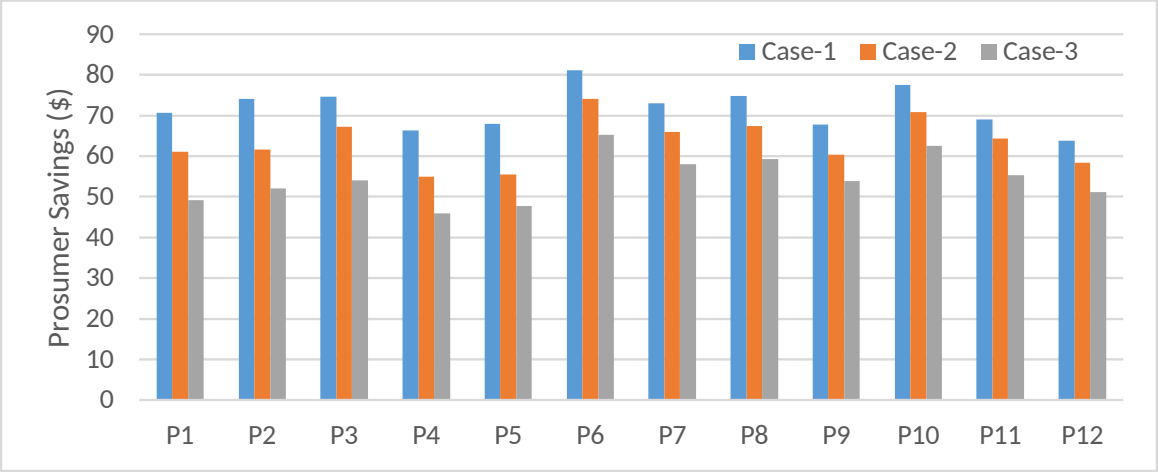

Figure 3.13: Prosumer Aggregated Savings

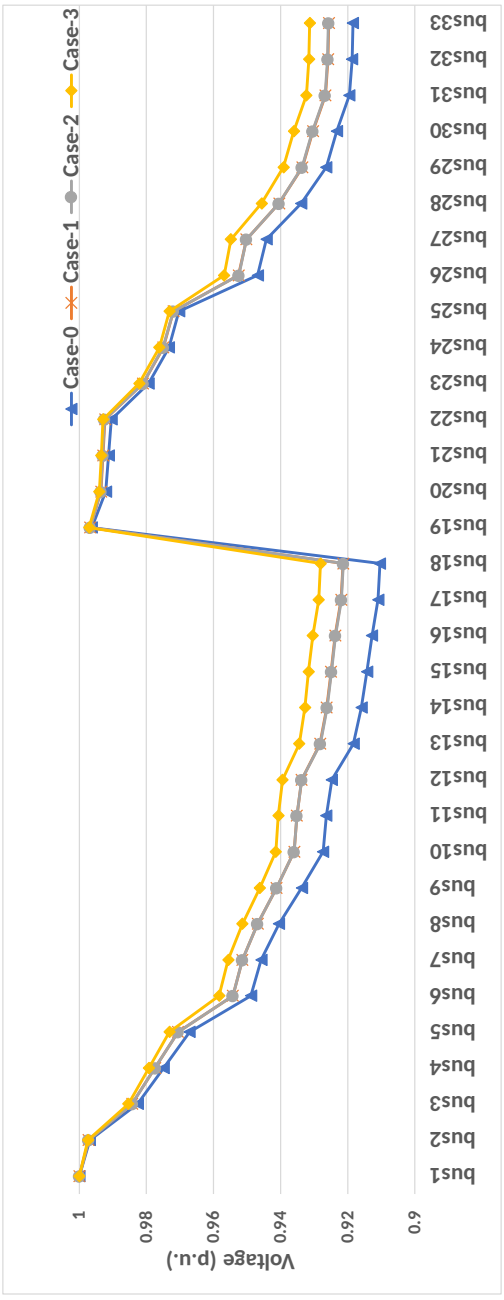

Figure 3.14: Feeder voltage profile at 13:00 hour, for different cases

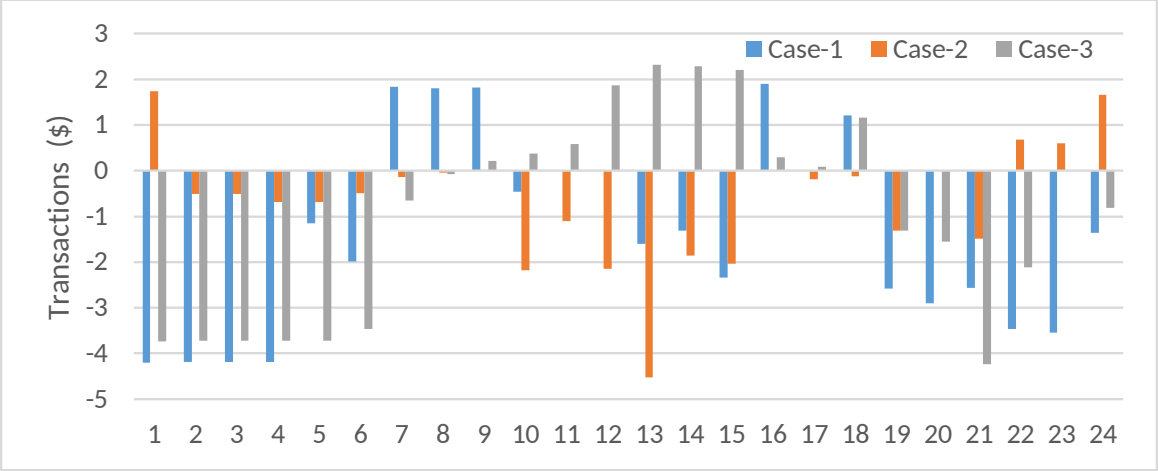

Figure 3.15: Prosumer P1 (With ESS) financial transactions

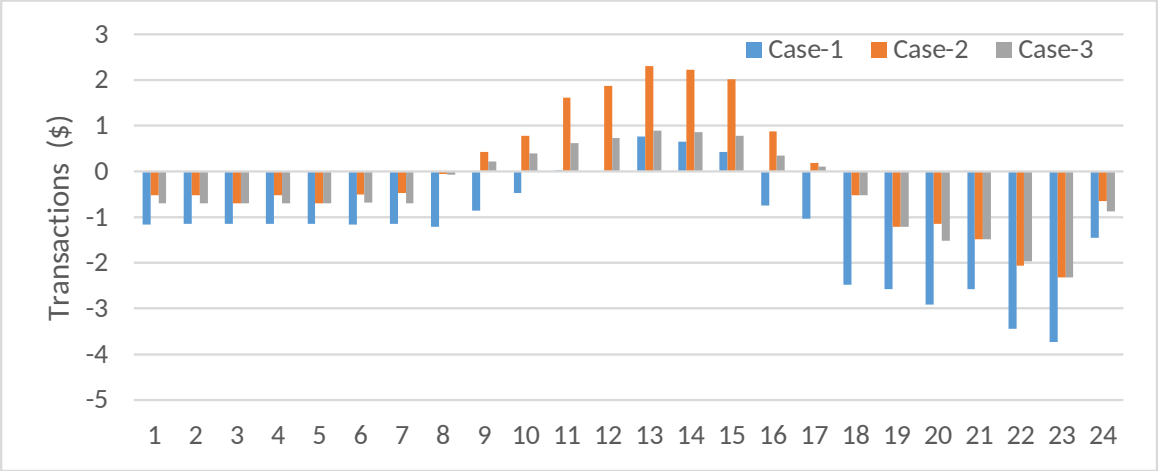

Figure 3.16: Prosumer P6 (Without ESS) financial transactions

Chapter 4

An MPC based Approach for the Proposed Multi-Layer P2P Energy Trading Framework Considering Uncertainties

4.1 Introduction

In Chapter 1 of this thesis the flexibility of the proposed multi-layer framework was discussed in terms of its compatibility with different transactive energy strategies. The framework was then developed in Chapter 3 where the simulation results demonstrated its usefulness in grid support and prosumer operational planning. This framework has its limitations however, since the prosumer operation is planned without considering the uncertainties that may occur in a practical system. As a result, the prosumers are unable to respond to system disturbances or deviations. This chapter resolves these limitations by extending the framework through an MPC based approach which further facilitates operational flexibility of a prosumer and ensures dynamic prosumer operations, i.e. the ability of a prosumer to dynamically adjust its status from a seller to a buyer or vice versa, based on both unpredictable and predictable variations in internal prosumer/external market conditions.

4.2 Mathematical Model

4.2.1 Changing Forecast and Actual Values

The accuracy of a forecast depends to a significant degree, on the time gap from when the forecast is being generated to when a parameter is being forecasted. This accuracy increases as the gap is decreased. In the present study, the two forecasted parameters used to analyze prosumer operation under uncertainties are; a) PV generation ($P_{i,t}^{PV}$) b) Grid electricity price (π_t^{G2P}) . For each of these parameters a new forecast is available at each hour, for the next 24 hours. These forecasts are shown as follows.

$$\mathbf{P_{i,tf}^{PV^{forecast}}} = \{P_{i,tf,1}^{PV^{forecast}}, P_{i,tf,2}^{PV^{forecast}}, P_{i,tf,3}^{PV^{forecast}}, ..., P_{i,tf,T}^{PV^{forecast}}\} \quad \forall i \in \mathcal{N} \ \forall tf \in \mathcal{T} \quad (4.1)$$

$$\boldsymbol{\pi}_{\mathbf{tf}}^{\mathbf{G2P^{forecast}}} = \{\pi_{tf,1}^{G2P^{forecast}}, \pi_{tf,2}^{G2P^{forecast}}, \pi_{tf,3}^{G2P^{forecast}}, ..., \pi_{tf,T}^{G2P^{forecast}}\} \quad \forall tf \in \mathcal{T} \quad (4.2)$$

where $\mathbf{P_{i,tf}^{PV^{forecast}}}$ and $\boldsymbol{\pi}_{\mathbf{tf}}^{\mathbf{G2P^{forecast}}}$ denote the forecast profiles generated at the hour tf respectively. Note that regardless of the hour at which the profiles are generated, each profile contains values forecasted for hours from $t = 1$ to $t = T$. The forecast for the values at hours from 1 to tf are actually for the next day due to the circular boundary assumed in this study as shown in Fig.2.2 and Fig.2.1. The actual profile of these parameters with no uncertainty, which is known at the end of the day, is given as follows

$$\mathbf{P_i^{PV^{actual}}} = \{P_{i,1}^{PV^{actual}}, P_{i,2}^{PV^{actual}}, P_{i,3}^{PV^{actual}}, ..., P_{i,T}^{PV^{actual}}\} \quad \forall i \in \mathcal{N} \quad (4.3)$$

$$\boldsymbol{\pi}^{\mathbf{G2P^{actual}}} = \{\pi_1^{G2P^{actual}}, \pi_2^{G2P^{actual}}, \pi_3^{G2P^{actual}}, ..., \pi_T^{G2P^{actual}}\} \quad (4.4)$$

Note that the forecast is generated by considering the "known" uncertainties and trend-forming aspects of historical data. There are also some "unknown" uncertainties considered in the present study which can cause *unforecastable* deviations. These can be explained by comparing the forecasts and the actual profiles of uncertain parameters. In Fig.4.1 the forecast of PV generation for prosumer 1 is shown to predict the actual profile with some

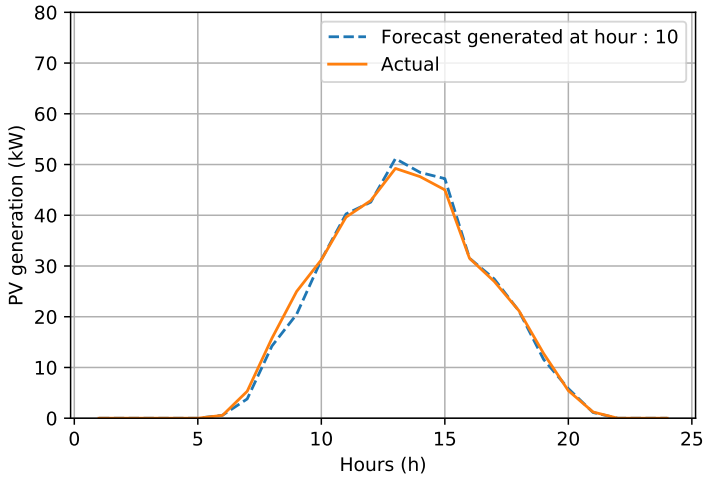

Figure 4.1: PV generation forecast generated at Hour 10 and actual profile for Prosumer 1

accuracy. The difference between the forecast and this actual value is the forecasting error and is considered to be a "known" uncertainty. The actual profiles shown in Fig.4.2 and Fig.4.3 show spikes occuring at Hour 13 and Hour 20 respectively. In both figures however, the generated forecasts do not predict these spikes; hence such unexpected occurrences are categorized as "unknown" uncertainties. Such deviations are not considered to be trend-forming so the forecasts generated after these events do not show any spike at the time where they previously occurred.

4.2.2 Model Predictive Control of a Multi-Layer P2P Energy Trading Framework

The MPC approach used in this study for the continual execution of the developed multi-layer P2P energy trading framework performs one optimization for each time interval. Before attempting to optimize the framework, all the up-to-date data regarding the prosumer environment, which in this study, comprises PV generation and grid power pricing, is used as input to the model at each time interval, along with some extra settings for prosumer ESS, which will be discussed in this section. At each interval, a new forecast for each of these parameters is generated as described in 4.1 and 4.2, and the actual values of these parameters at that interval as described in 4.3 and 4.4. Once the model is solved at

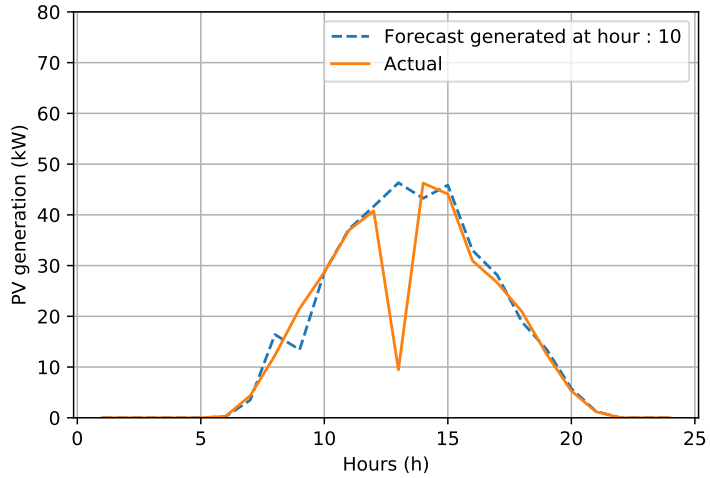

Figure 4.2: PV generation forecast generated at Hour 10 and actual profile for Prosumer 5

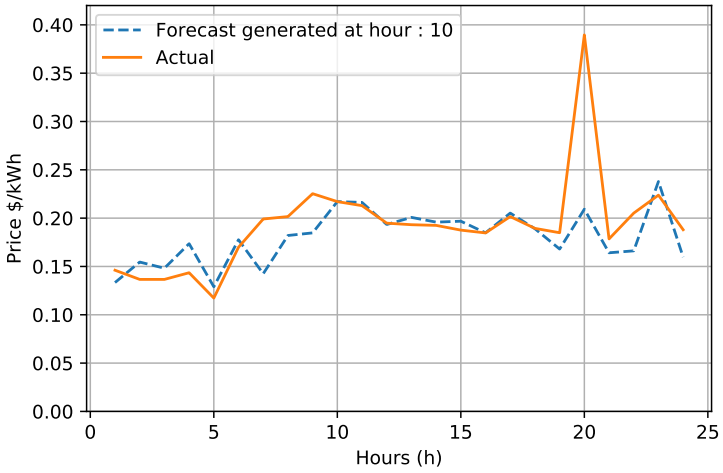

Figure 4.3: Hourly Ontario Energy Pricing (HOEP) forecast generated at Hour 10 and actual profile

a particular time interval, the prosumer decisions for that interval only, are applied, and all subsequent ones are discarded.

A receding horizon is considered in this thesis as the MPC optimization period. The reasoning behind this choice of a horizon is the manner in which the proposed multi-layer framework operates. This is explained by considering the market objective functions in 3.6, 3.7 and 3.8 which are summed up over the optimization horizon and can therefore be split into the current time interval and future time intervals, as explained with the following equations.

$$\text{Max } Welfare = \sum_{i \in \mathcal{N}} W_{i,tf_0}^{actual} + \sum_{i \in \mathcal{N}} \sum_{t=tf_0+1}^{tf_0+T-1} W_{i,t}^{forecast} \tag{4.5}$$

Here W_{i,tf_0}^{actual} is the prosumer welfare at the time interval tf_0 which is considered the present interval at which the real-time values of PV generation and grid power price are known and used to evaluate the welfare. $W_{i,t}^{forecast}$ is similarly the prosumer welfare for all the future time intervals for which the forecasted values are used. In 4.5 the total horizon length remains fixed, despite part of the formulation being real-time parameter values and part of it being forecasted values. Note that if the time instant tf is after the start of the day, the $(tf_0 + T - 1)$ value exceeds T. In such a case the optimization horizon goes into the next day and is wrapped around, as shown in Fig.2.2 and Fig.2.1. The benefit of this approach is that, in practice, the model developed in Chapter 3 does not need to be modified and can be used as a 'blackbox' where only the inputs are changed before each optimization. The algorithm for this MPC approach is given below for the case where the system is simulated with generated data.

Algorithm 1: Model Predictive Control of the Multi-Layer P2P Energy Trading Framework

input : $\mathbf{P_{i,tf}^{PV^{forecast}}}, \boldsymbol{\pi}_{\mathbf{tf}}^{\mathbf{G2P^{forecast}}}, \mathbf{P_{i}^{PV^{actual}}}, \boldsymbol{\pi}^{\mathbf{G2P^{actual}}}$
output: MPC prosumer operation
Reset all variables and marginals;
for *each* $tt \in \mathcal{T}$ **do**
  Set $P_{i,t}^{PV} \leftarrow P_{i,tt,t}^{PV^{forecast}} \quad \forall i \in \mathcal{N} \ \forall t \in \{\mathcal{T} \mid t \neq tt\}$;
  Set $P_{i,tt}^{PV} \leftarrow P_{i,tt}^{PV^{actual}} \quad \forall i \in \mathcal{N}$;
  Set $\pi_{t}^{G2P} \leftarrow \pi_{tt,t}^{G2P^{forecast}} \quad \forall t \in \{\mathcal{T} \mid t \neq tt\}$;
  Set $\pi_{tt}^{G2P} \leftarrow \pi_{tt}^{G2P^{actual}}$;
  if *tt is not first element of* $\mathcal{T}$ **then**
    Fix Variable $E_{i,tt}^{(\text{Current Iteration})} = E_{i,tt}^{(\text{Previous Iteration})}$;
  end
  Optimize selected Multi-Layer P2P Framework objective;
  MPC prosumer operation at $tt \leftarrow$ Prosumer decisions at tt after optimization ;
  Reset all variables and marginals;
end

This algorithm can easily be extended to practical system operation with close to real-time decisions by adjusting the duration of the time interval and setting up a continuously running loop. In this continuous mode of operation the real-time data on RES generation and grid power price, along with their updated forecasts at each time interval, would be required. Note that the SOC variable of the ESS obtained for interval tt will remain fixed in the next iteration as the MPC progresses, since it is the only variable having temporal and circular boundary constraints.

4.3 Implementation and Results

The parameter profiles considered in Chapter 3 for prosumer PV generation, prosumer base consumption (Fig.3.4) and grid electricity buying/selling prices are again used in this chapter to ensure a consistent simulation environment so that the contrast between the MPC approach used here and the deterministic approach of the previous chapter can be accurately studied. The number of prosumers, their physical placement on the 33 bus distribution feeder and the fixed non-participating loads have been kept the same for

this reason as well. All case studies presented in this chapter consider only the welfare maximization objective to evaluate prosumer response to the various cases of uncertainties because it presents the most likely mode of prosumer operation as it incentivizes prosumers to improve their satisfaction while lowering their energy costs.

In order to simulate uncertainty in forecast, actual parameter profiles are scaled randomly based on the hour at which the forecast is required. For the 24 hour horizon with 1 hour intervals, 24 forecasts have been generated for each of the PV generation and grid power price profiles. This is accomplished by varying the upcoming values at each hour by a random percentage, which increases the further away the forecast is from the current hour and reaches a maximum of $\pm 40\%$ when the forecasted value is 24 hours away. Note that Fig.4.1, Fig.4.2 and Fig.4.3 all show the forecast generated at Hour 10 compared to their actual profiles. In these figures the forecast immediately after Hour 10 is much more accurate than the forecast immediately before it, because the forecast at Hour 9 is for the next day which is 23 hours away, resulting in very high uncertainty.

Three cases are developed for simulations; in **Case-1**, only uncertainty in PV generation ($P_{i,t}^{PV}$) is considered, while a subset of prosumers experience an unexpected sudden loss of PV generation. The PV generation profile and forecast for an unaffected prosumer is shown in Fig.4.1 while Fig.4.2 shows the profile for a prosumer that is experiencing the unexpected outage in PV generation at Hour 13. Note that the forecast at Hour 10 did not predict the dip in generation, indicating that this disturbance was not predictable from historical trends. In this thesis only the prosumers P5, P6, P7 and P8 experience this PV generation outage. All affected prosumers experience an 80% reduction in PV generation capacity at Hour 13 and among them only P5 possesses an ESS. The TOU tariff, as considered in the previous chapter is used in this case and the simulation results obtained with uncertain PV generation are compared with those of deterministic generation assumed in Chapter 3.

For the **Case-2**, only the power purchase price from the grid (π_t^{G2P}) is considered to be uncertain with an unexpected spike occurring at Hour 20, while the PV generation is assumed to be deterministic and without uncertainty. Hourly Ontario Energy Price (HOEP) data from 8th September 2020 is used to generate the forecasts in the same manner as described earlier. The actual HOEP profile is generated simply by introducing a spike at Hour 20 to the original data and can be seen in Fig.4.3 along with the forecast profile obtained at Hour 10. All prosumers are affected in this case since the price set by the grid applies to every prosumer. Similar to the first case, the price spike is not predictable and the forecast at Hour 10 shown in Fig.4.3, is generated without the knowledge of such an event to occur. Two sets of results are generated by simulation for this case for comparison; one where an unexpected spike occurs at hour 20 and one with no such occurrence.

Case-3 is simply the combination of the first two cases where uncertainty for both, the PV generation and the grid electricity price is considered. The unexpected deviations from the above cases comprising of the outage in PV generation at Hour 13 and the spike in price at Hour 20 are seen by prosumers. Similar to the second case, two sets of results are generated for comparison; one where both the unexpected deviations occur in the system and one where the actual profiles have no such deviation.

4.3.1 Case-1: Uncertainties in PV Generation

The behavior of prosumers in this case appears to be significantly close to their response in Chapter 3 for the welfare maximization objective. Note that the prosumers are charging their ESS during the early off-peak hours of the day as seen in Fig.4.4. Since there is no PV generation at this time, the energy for self-consumption and charging is purchased from the grid (Fig.4.5). At Hour 7, the mid-peak pricing takes effect and the prosumers collectively stop purchasing power from the grid to engage in P2P energy trade to meet their self-demand until they become self-sufficient in their PV generation at Hour 11. This behavior is again seen during the next mid-peak period from Hour 16 to Hour 18 where prosumers with ESS discharge their batteries to participate in the P2P market. The magnitude of power that prosumers are purchasing from the P2P market is shown in Fig.4.6, which indicates a pattern of P2P energy trade similar to that of the deterministic case in Chapter 3 (Fig.3.6).

The only exception in the MPC case however, is the unexpected PV generation dip occurring for some prosumers at Hour 13. Note that even during this dip, there is no power purchased from the grid, which implies that the prosumers are meeting their power deficit by either purchasing power from the P2P market or by discharging their own ESS. This is evident from Fig.4.6 where a highly noticeable spike in P2P power exchange is seen at Hour 13 which has resulted from the reduced PV generation. Normally, during the peak generation hours the trend of P2P power exchange is reversed since all the prosumers are self-sufficient in their PV genertion, and all the available power surplus is being sold to prosumers with ESS to charge their batteries which are subsequently discharged again in the mid-peak hours.

This behavior of charging ESS from PV generation surplus can be seen from the heatmaps in Fig.4.7 at Hour 15 which also shows the P2P exchanges occurring at Hour 13 during the generation dip. Note that the prosumers P6, P7 and P8 purchase a significant portion of their power from prosumers with ESS, suggesting that thes prosumers with ESS are discharging their batteries to sell power in the P2P market; a behavior that is usually

Table 4.1: Case-1: Comparison of MPC based and deterministic P2P energy trade considering PV uncertainty

Variables \ Cases	Deterministic PV Generation	With PV uncertainty	
		w/ MPC	w/o MPC[1]
Total Welfare ($)	5842	5815	5839
Total Power Loss (p.u.)	0.224	0.224	0.224
Total Prosumer Power Cost ($)	360	376	361
Total PV Generation (kWh)	4699	4541	4679
Total Energy bought from Grid (kWh)	3537	3676	3548
Total Prosumer Consumption (kWh)	8059	8010	8045
Total P2P Exchange (kWh)	541	543	558
Total Energy Sold Sold to Grid (kWh)	0	0	0

[1] Based on the forecasts generated at Hour-1

seen during the mid-peak hours for the welfare maximization objective (Fig.4.7 Hour 9 and Hour 15). A comparison of the various system parameters for this case and the deterministic welfare maximization case of Chapter 3 is presented in Table.4.1. It is seen that the reduced PV generation results in an increase in prosumer energy cost, despite no power being purchased from the grid during the hour of the deviation. This increase is attributed to the the power purchases from the grid during the off-peak hours after the deviation has occurred, which are made to charge the depleted ESS batteries.

4.3.2 Case-2: Uncertainties in Hourly Ontario Energy Price (HOEP)

In this case the prosumer responses are similar in some respects to Case-1 because the HOEP profile (Fig.4.3) can also be categorized in a manner similar to the TOU pricing scheme i.e. the off-peak hours (Hour 1 - Hour 6), the mid-peak hours (Hour 7 - Hour 19 , Hour 21 - Hour 24), and the on-peak hours (Hour 20). As in Case-1, the prosumers in this

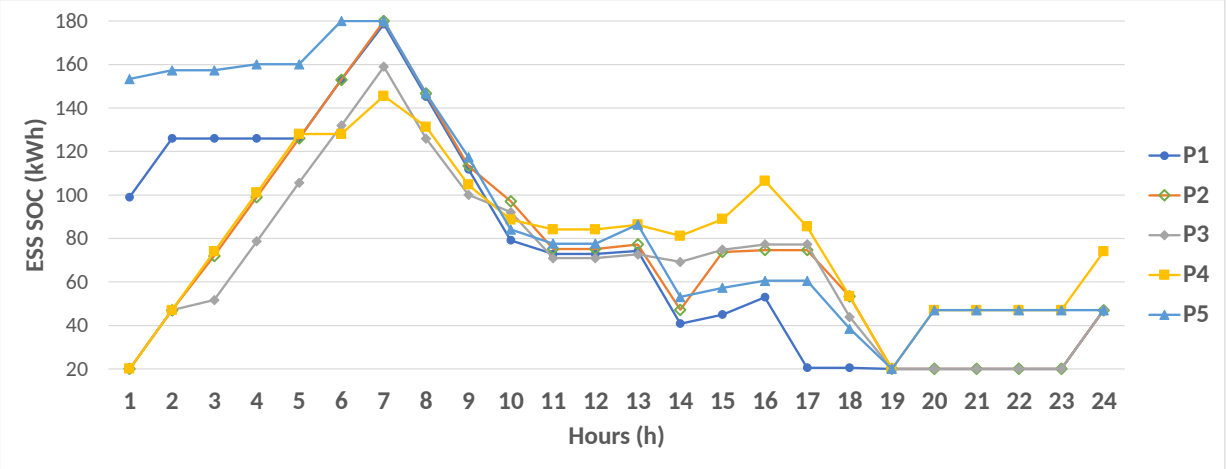

Figure 4.4: Case 1: SOC of prosumer ESS

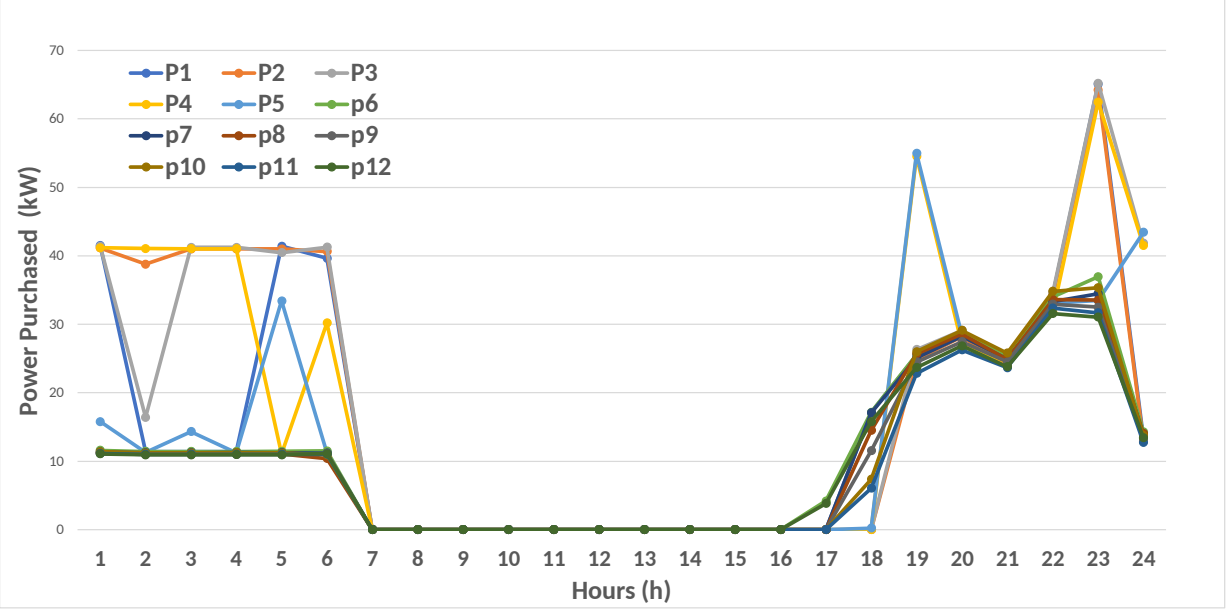

Figure 4.5: Case 1: Grid power purchased by prosumers

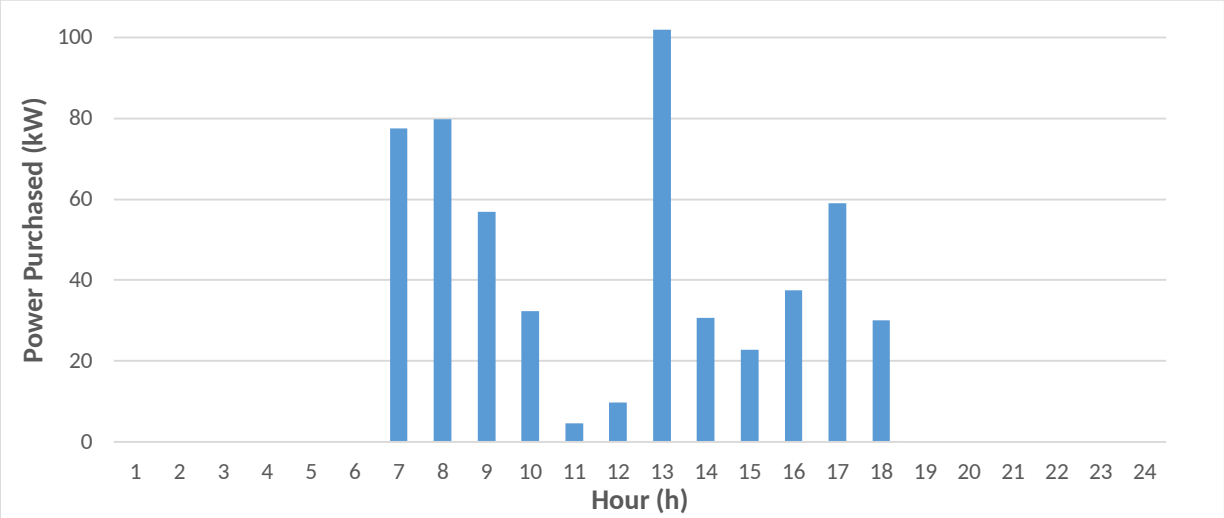

Figure 4.6: Case 1: P2P power purchased by prosumers

case also begin purchasing a significant amount of power during the early off-peak hours to charge their ESS which can be seen from their SOC in Fig.4.8 and Fig.4.9. The prosumers with ESSs then discharge their batteries to participate in the P2P market as the HOEP starts increasing at Hour 8. At this point, the PV generation of all prosumers is sufficient enough for them to stop grid purchases, as shown in Fig.4.10 and Fig.4.11. The energy purchased by prosumers from the P2P market can be seen in Fig.4.12 and Fig.4.13; this is not a complete picture, however, since the trend of the exchange is not apparent from the gross quantity exchanged. These trends can be gleaned from the hourly heatmaps of P2P exchange, in Fig.4.16. It is noted that the prosumers with ESS sell power to those prosumers that have none at Hour 8; the trend is then reversed by Hour 13 as the PV generation surpasses prosumer self-demand, at which point the surplus is purchased back to charge the ESS batteries. This trend is then again reversed by Hour 17 as the PV generation falls.

Note that for each of the prosumer responses there are two plots referenced for this case; one in which the prosumer experiences the unexpected HOEP spike, and one where there is no such occurrence. Since the unexpected spike occurs late (at Hour 20), all the prosumer behaviors prior to this point are exactly the same. At Hour 20 the prosumers with ESS, predictably start discharging their batteries to sell power in the P2P market despite there being no PV generation at this time. Moreoever, the prosumers reduce their consumption as a response to the increase in price as shown in Fig.4.14 and Fig.4.15. A numerical

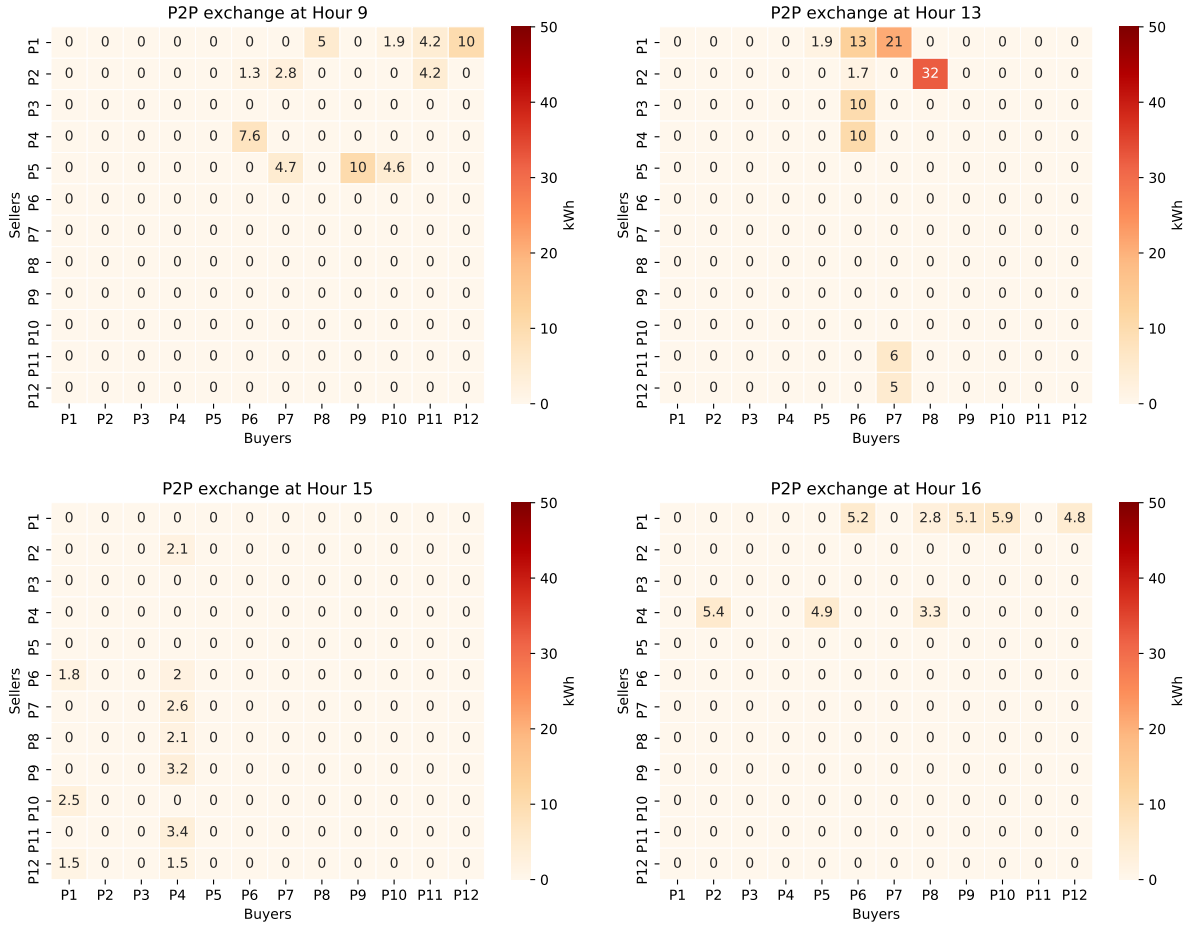

Figure 4.7: Case-1: Notable heatmaps for P2P exchange

Table 4.2: Case-2: Comparison of MPC Prosumer responses considering HOEP uncertainty

Variables \ Cases	First Hour Forecast	With HOEP uncertainty	
		w/ spike	w/o spike
Total Welfare ($)	5636	5596	5613
Total Power Loss (p.u.)	0.2220	0.2211	0.2216
Total Prosumer Power Cost ($)	512	532	534
Total PV Generation (kWh)	4699	4699	4699
Total Energy bought from Grid (kWh)	3247	3089	3195
Total Prosumer Consumption (kWh)	7801	7642	7707
Total P2P Exchange (kWh)	321	476	426
Total Energy Sold Sold to Grid (kWh)	0	0	0

comparison is presented in Table.4.2 where the energy cost for the prosumers is shown to not be significantly affected in the event of an unexpected price spike. This outcome is attributed to the higher volume of P2P energy exchanges and reduced consumption by prosumers responding to the price spike.

4.3.3 Case-3: Uncertainties in PV Generation and HOEP

This case combines the uncertainties considered in the previous two cases in a single simulation to study the prosumer behavior when both the PV generation, and the grid power price are uncertain. It can be inferred that the prosumers will respond in a manner similar to how they did in the previous two cases. In the interest of efficiency, in this section only the prosumer responses during the disturbances (PV generation dip at Hour 13 and grid power price spike at Hour 20), will be analyzed in detail. Prosumer behaviors during the other hours when the system is not experiencing any disturbances, can be understood by comparing the prosumer operational figures for this case and linking them with the explanations given in the previous two cases.

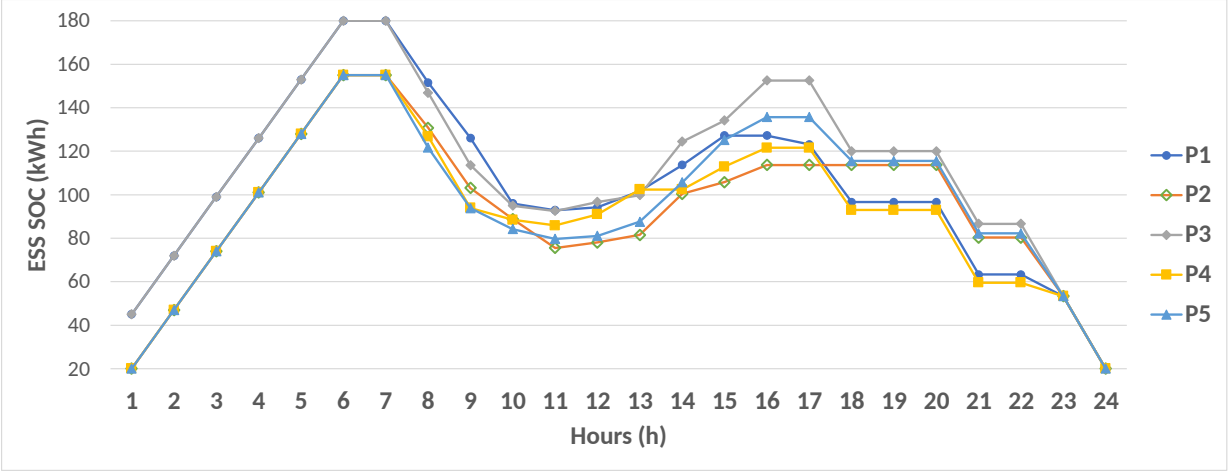

Figure 4.8: Case 2: SOC of prosumer ESS w/ HOEP spike

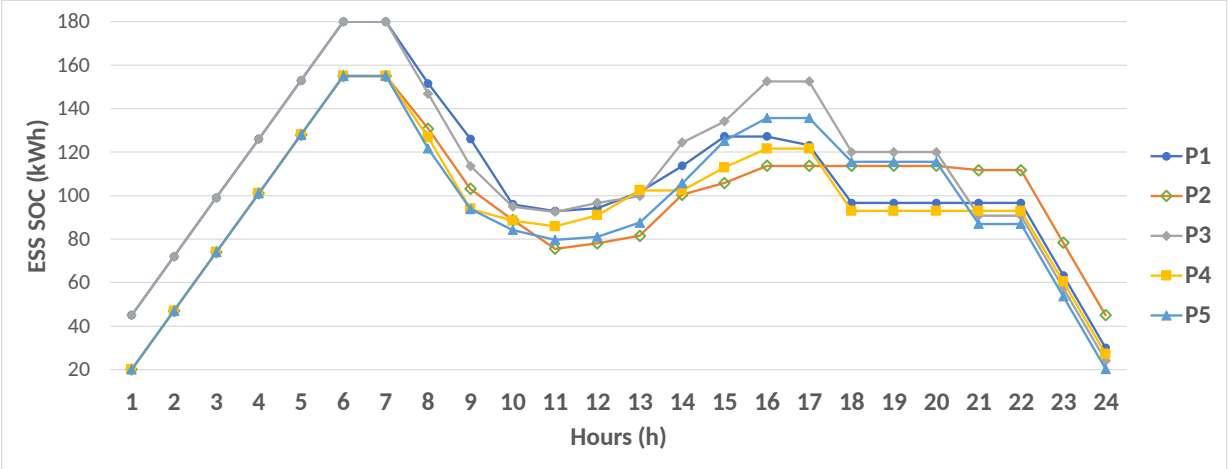

Figure 4.9: Case 2: SOC of prosumer ESS w/o HOEP spike

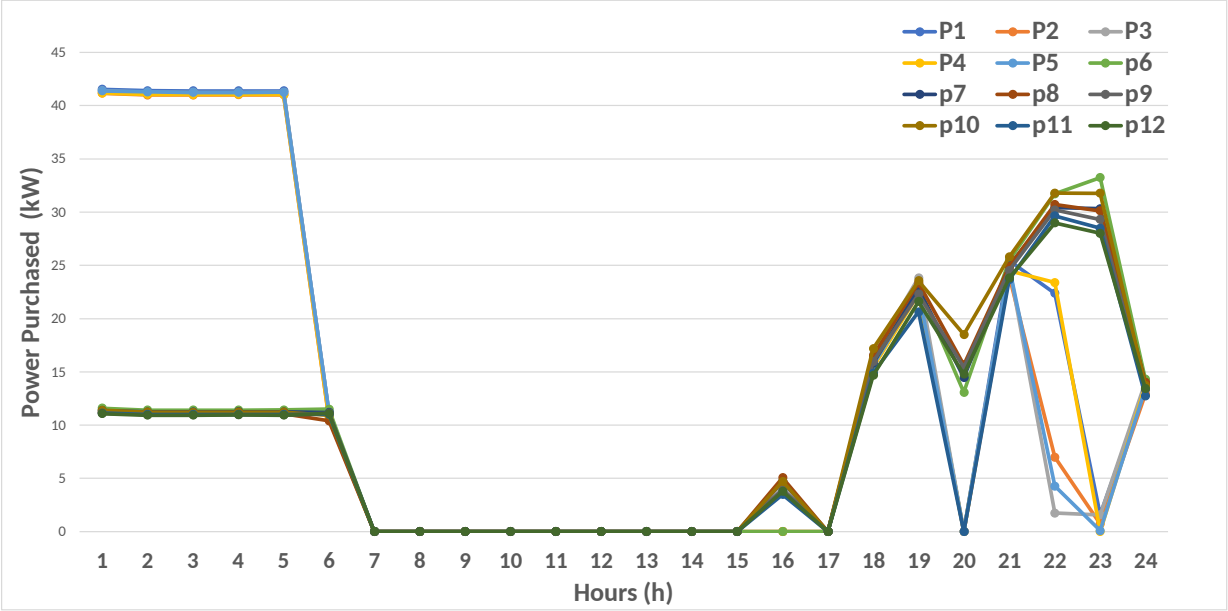

Figure 4.10: Case 2: Grid power purchased by prosumers w/ HOEP spike

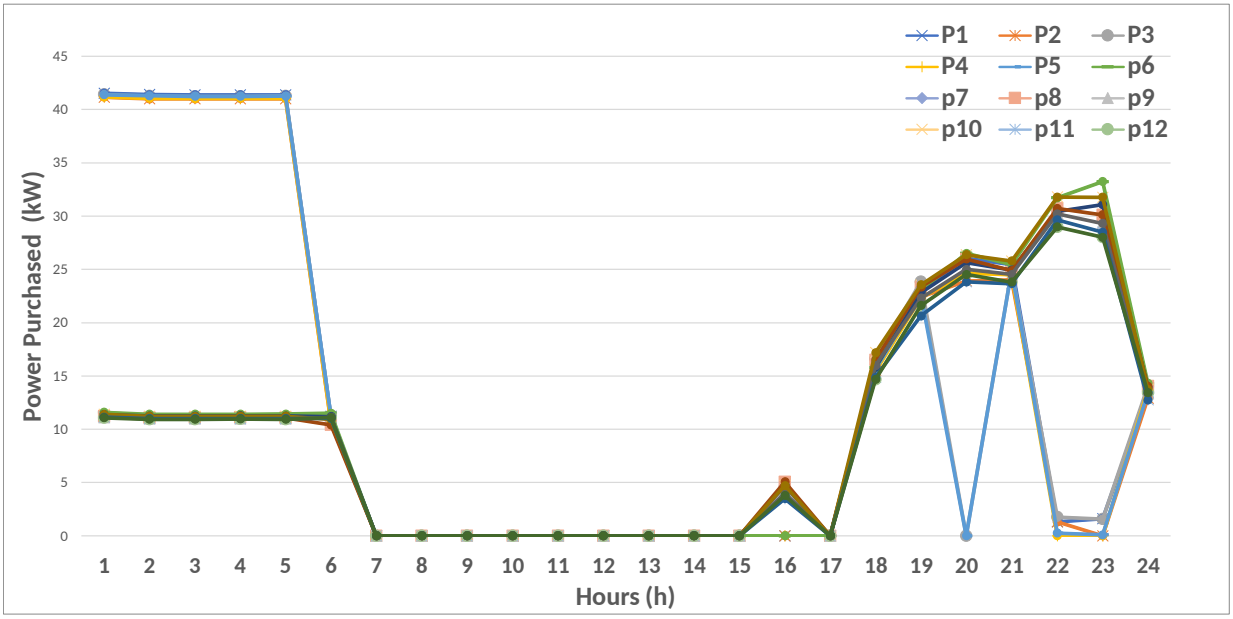

Figure 4.11: Case 2: Grid power purchased by prosumers w/o HOEP spike

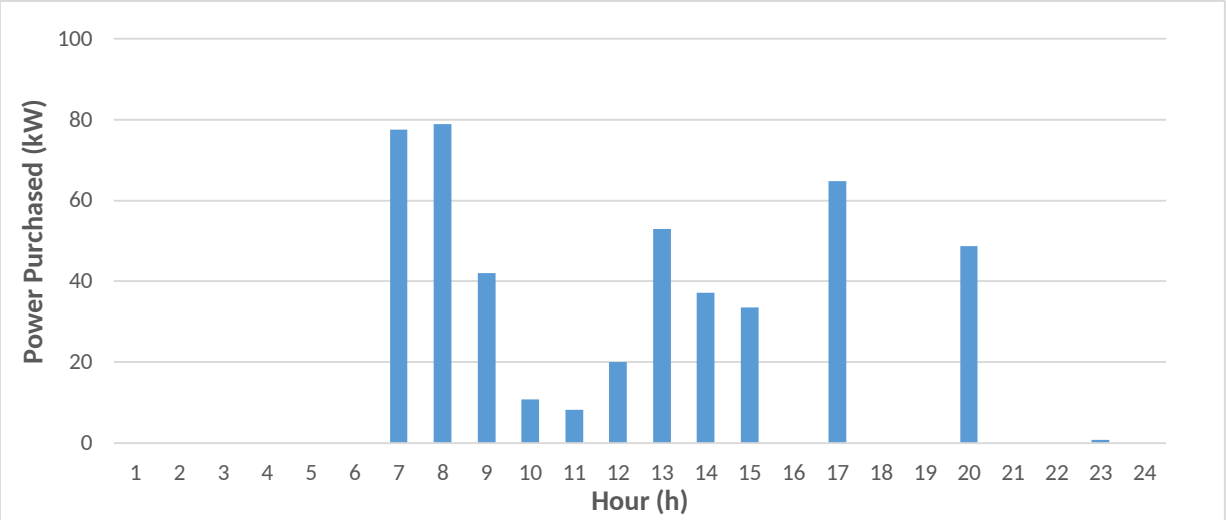

Figure 4.12: Case 2: P2P power purchased by prosumers w/ HOEP spike

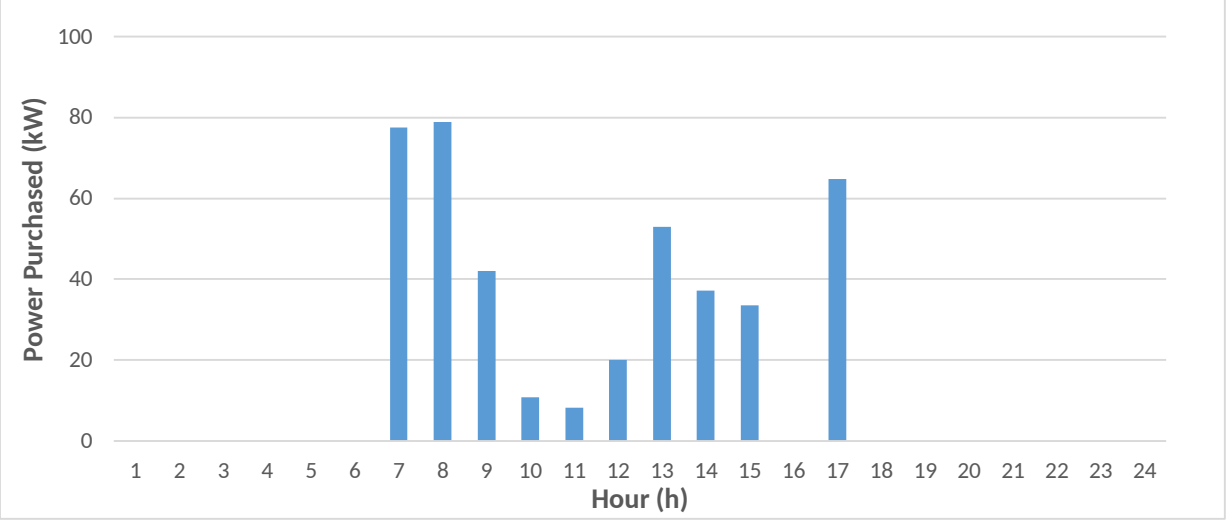

Figure 4.13: Case 2: P2P power purchased by prosumers w/o HOEP spike

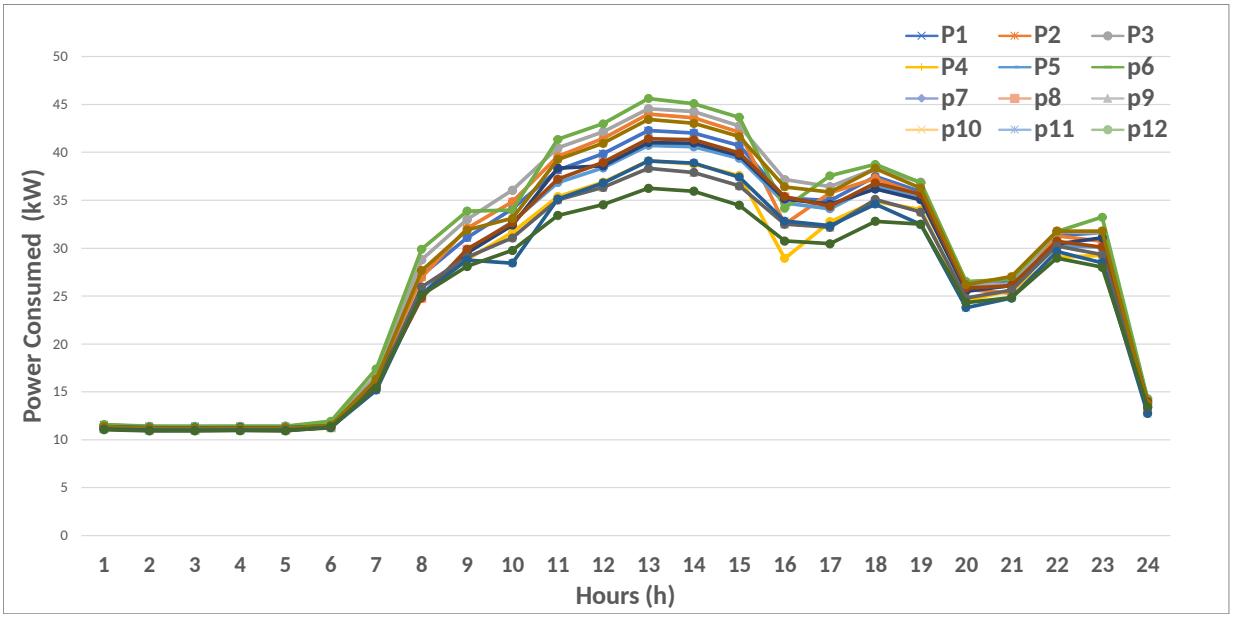

Figure 4.14: Case 2: Power consumed by prosumers w/ HOEP spike

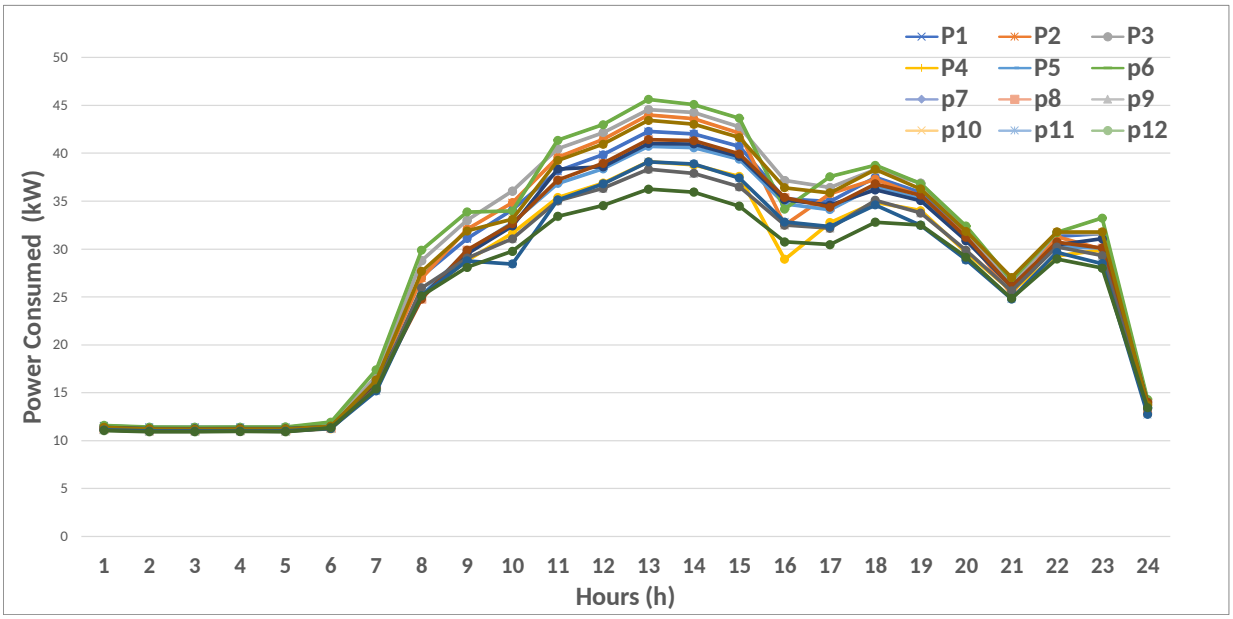

Figure 4.15: Case 2: Power consumed by prosumers w/o HOEP spike

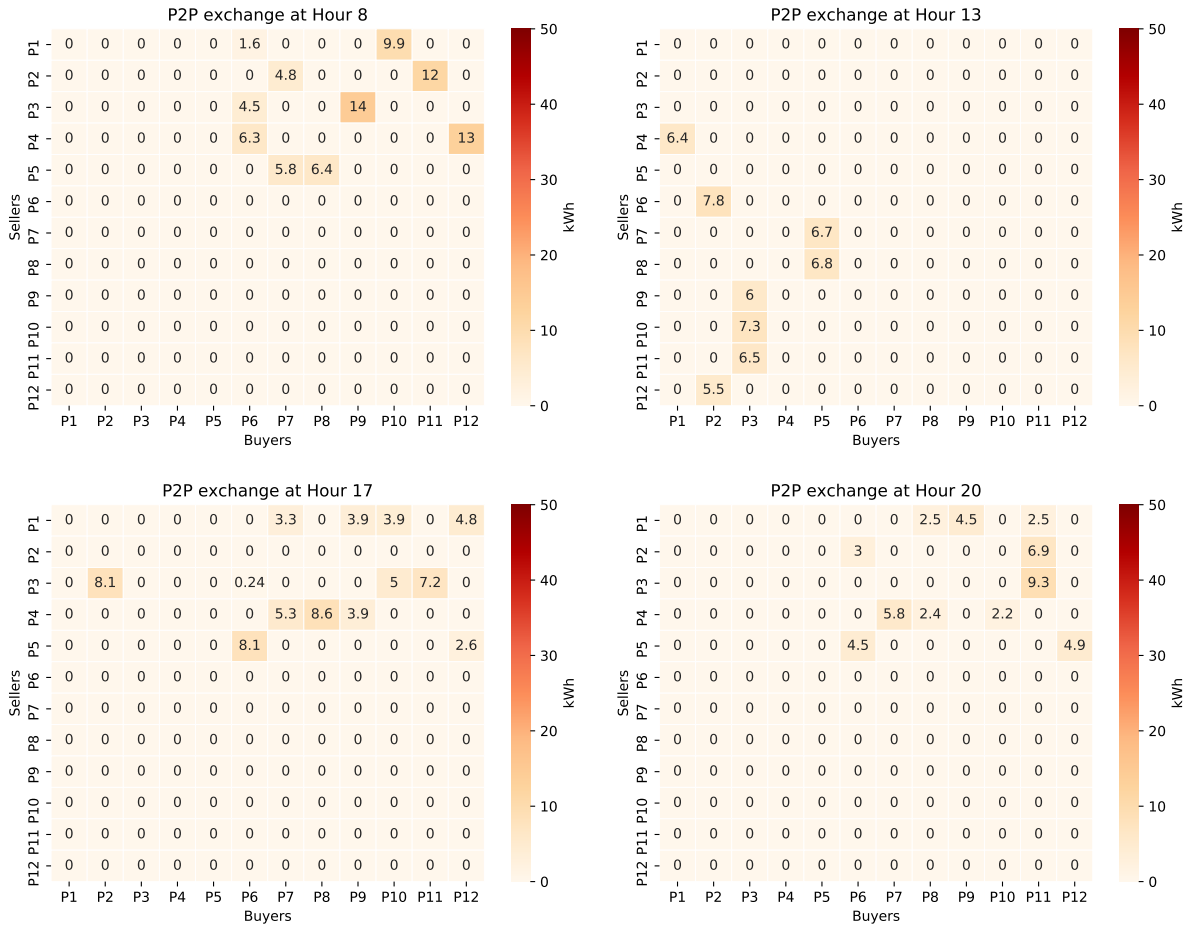

Figure 4.16: Case-2: Notable heatmaps for P2P exchange

The first disturbance occurring in this system is that of the PV generation dip at Hour 13. Note that if this disturbance had not occurred (Fig.4.18), the prosumers with ESSs would have charged their batteries with PV generation surplus at this hour. Instead the SOC remains unchanged (Fig.4.17) in a contrast to Case-1 where this SOC was significantly lower after Hour 13 (Fig.4.4). This is attributed to the HOEP pricing used in this case, where Hour 13 is considered to be similar to a 'mid-peak pricing', compared to the ToU pricing of Case-1 where Hour 13 was in the on-peak pricing interval. Due to this pricing difference, some of the affected prosumers elect to purchase the power deficit from the grid instead of the P2P market, as shown in Fig.4.19, such purchases would not have been made in the absence of this disturbance (Fig.4.20). The second disturbance occurs at Hour 20 and is a spike in the grid power price. This deviation incentivizes prosumers to engage in P2P energy trade to reduce their reliance on the grid as seen in Fig.4.21. Note that, in this figure, the P2P exchange at Hour 20 is less than the power exchanged at Hour 17 which can also be seen in the P2P exchange heatmaps at these hours (Fig.4.25), even though the ESS discharge at Hour 20 is higher than it is at Hour 17 (Fig.4.17). This outcome is seen due to the prosumers with ESS, first meeting their own self-demand, and then selling the rest of the power in the P2P market. The high P2P exchange at Hour 17 is not dependent on the forecast deviations and is also present if the system is simulated without them as seen in Fig.4.22. This exchange is attributed to the small local maxima occurring in the HOEP profile (Fig.4.3) which is forecasted by the prosumers. Moreover, the prosumers also react to reduce their own consumption at Hour 20 in response to the spike in grid power price as seen in Fig.4.23; a response identical to the one seen in Case-2.

The numerical values of system parameters for simulations, both with and without the unexpected deviations, are presented in Table.4.3. Note that the cost of energy purchased from the grid is noticeably higher for a system experiencing unexpected disturbances. This higher cost is associated with more energy purchased from the grid during the PV generation dip, and the power purchases made during the hour of the HOEP spike. The higher P2P exchange and lower consumption among the prosumers is expected from the results and is also seen in the previous cases.

4.3.4 Overview and Discussion

In all the cases developed in this chapter, the prosumers have been directed by the welfare maximization objective described in (3.6). The similarities in prosumer behaviors across these different cases are attributed to this same objective being used and can be seen in the results of Chapter 3 as well. The most notable among these behaviors is that of the prosumers charging their ESS early on in the day when the price of power is low as seen in

Table 4.3: Case-3: Comparison of MPC Prosumer responses considering HOEP and PV Generation uncertainty

Variables \ Cases	First Hour Forecast	With HOEP + PV Generation uncertainty	
		w/ outage + spike	w/o outage + spike
Total Welfare ($)	5649	5560	5611
Total Power Loss (p.u.)	0.2222	0.2233	0.2214
Total Prosumer Power Cost ($)	515	569	534
Total PV Generation (kWh)	4679	4541	4699
Total Energy bought from Grid (kWh)	3296	3275	3199
Total Prosumer Consumption (kWh)	7749	7641	7701
Total P2P Exchange (kWh)	492	470	427
Total Energy Sold Sold to Grid (kWh)	0	0	0

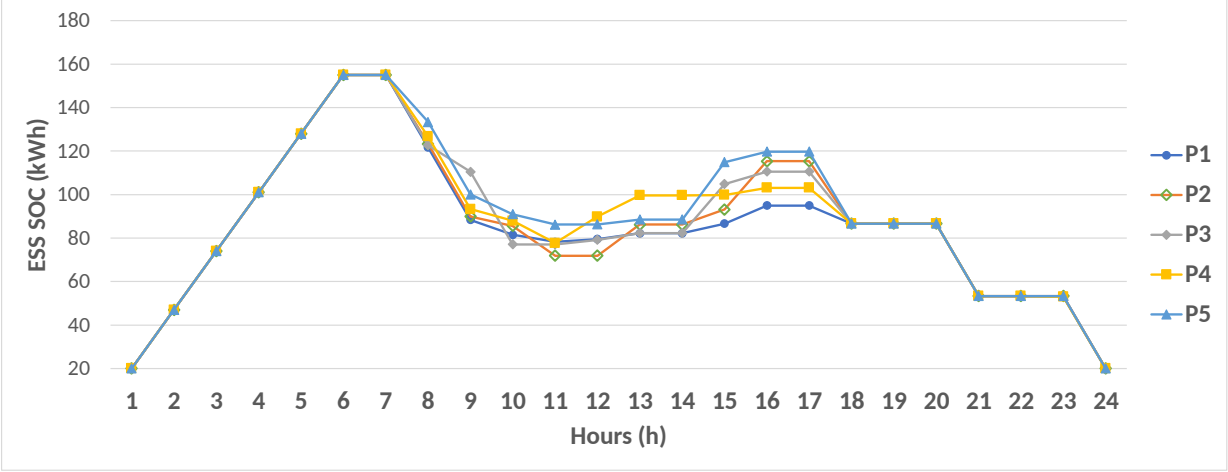

Figure 4.17: Case 3: SOC of Prosumer ESS w/ PV Generation dip and HOEP spike

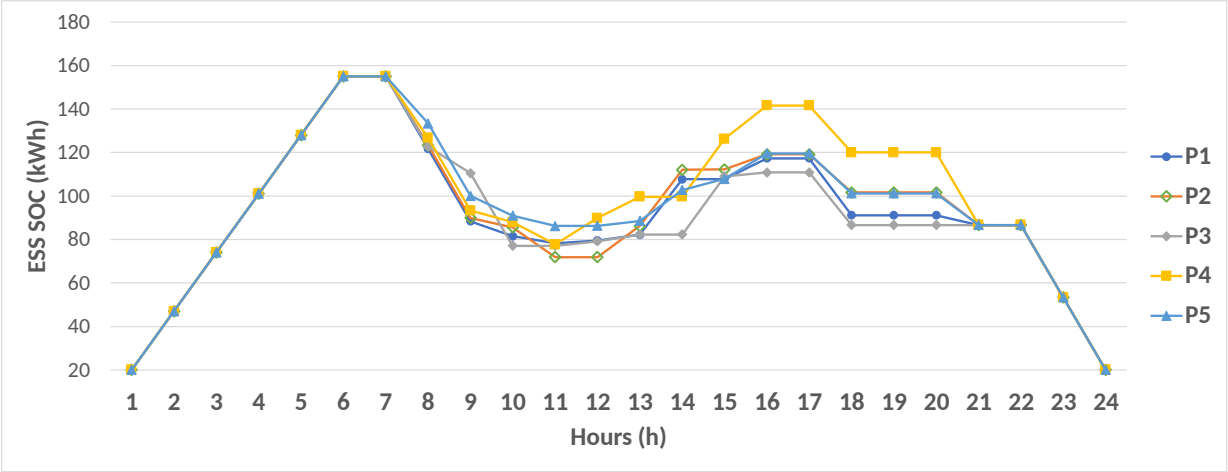

Figure 4.18: Case 3: SOC of Prosumer ESS w/o PV Generation dip and HOEP spike

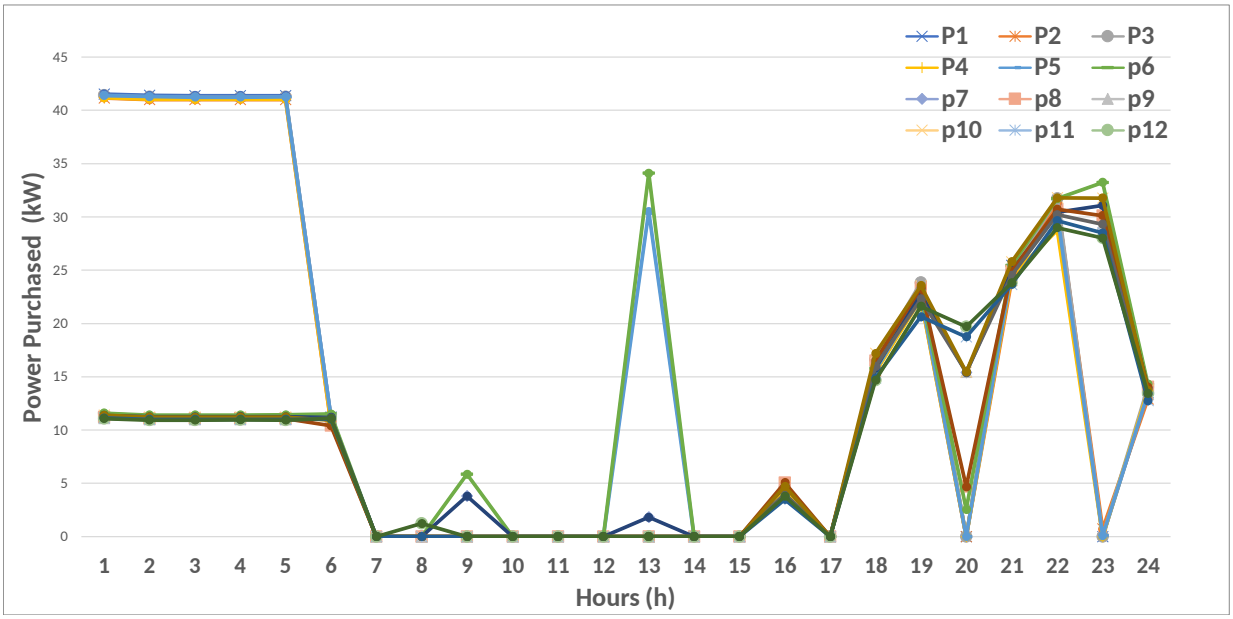

Figure 4.19: Case 3: Grid power purchased by prosumers w/ PV Generation dip and HOEP spike

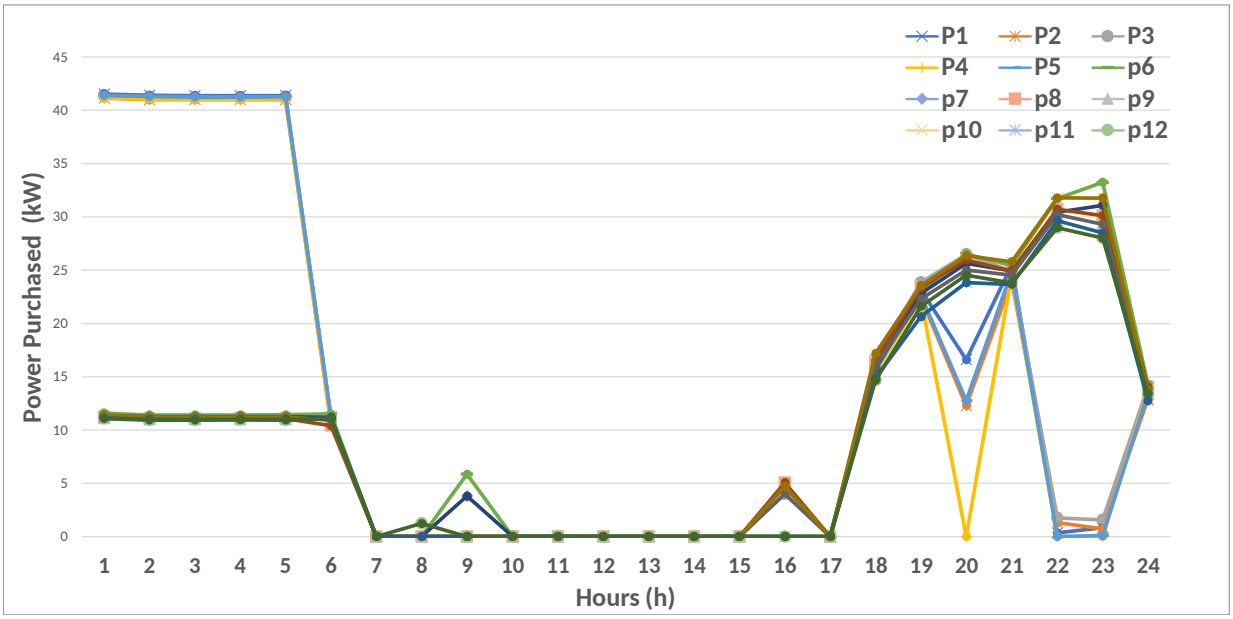

Figure 4.20: Case 3: Grid power purchased by prosumers w/o PV Generation dip and HOEP spike

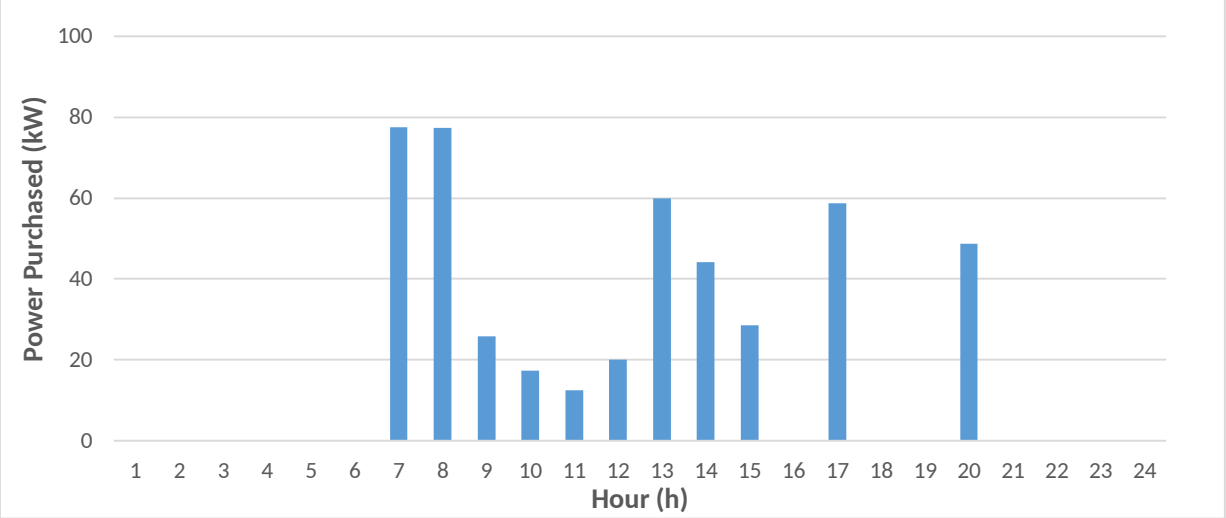

Figure 4.21: Case 3: P2P power purchased by prosumers w/ PV Generation dip and HOEP spike

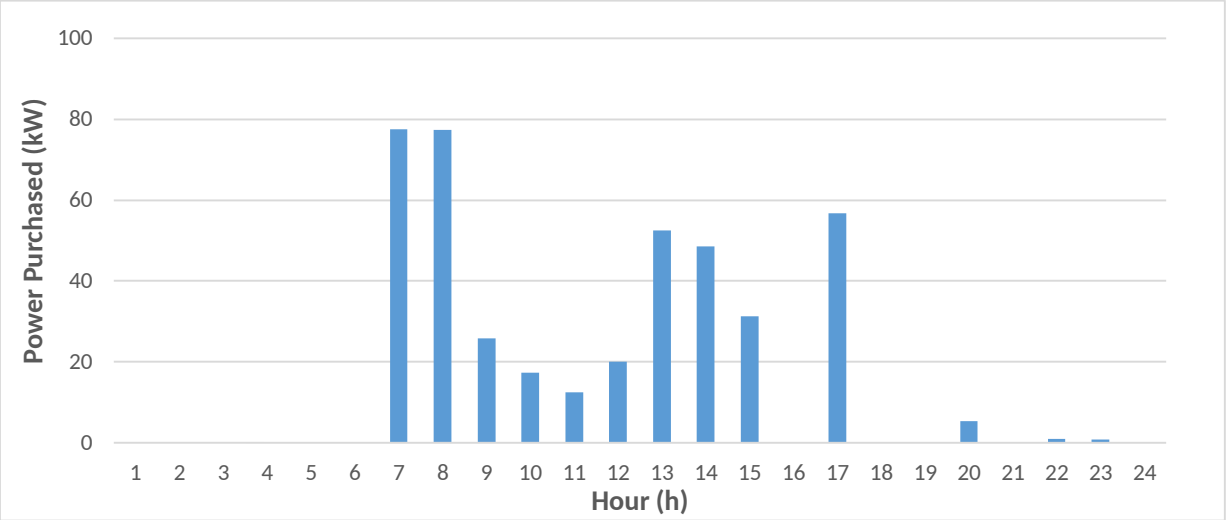

Figure 4.22: Case 3: P2P power purchased by prosumers w/o PV Generation dip and HOEP spike

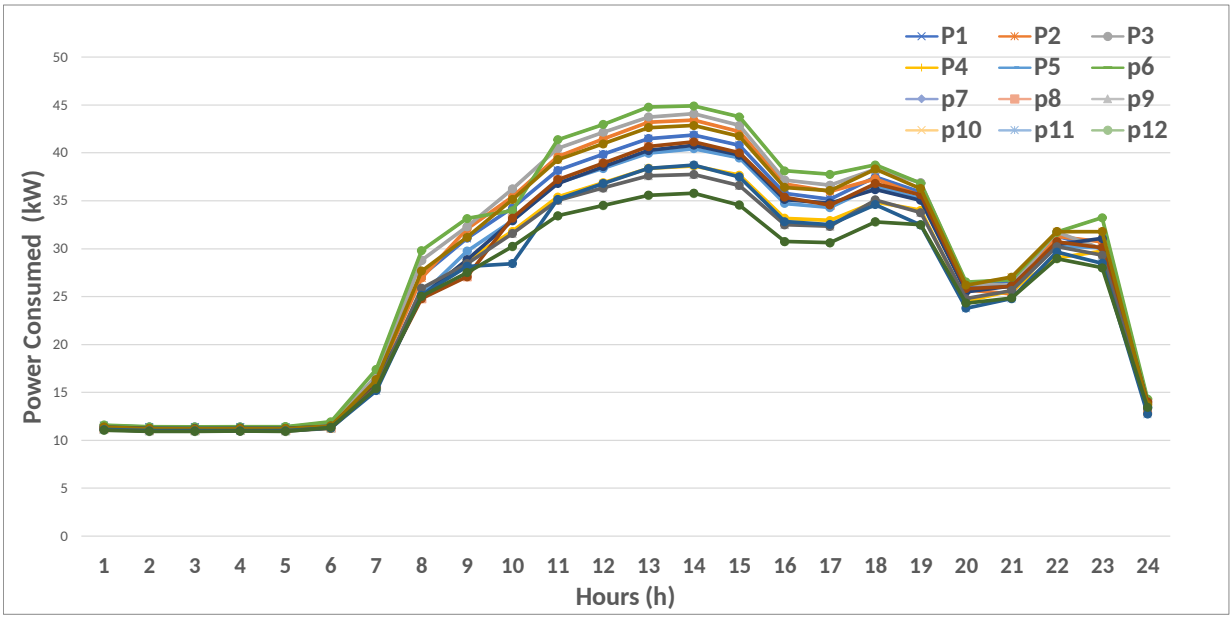

Figure 4.23: Case 3: Power consumed by prosumers w/ PV Generation dip and HOEP spike

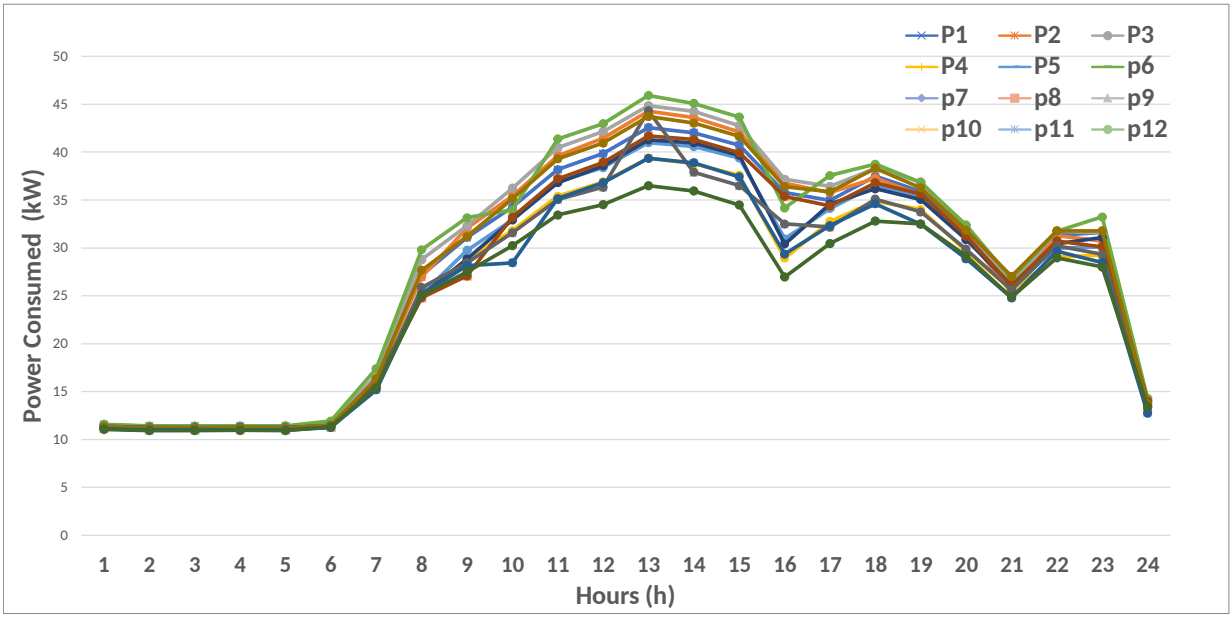

Figure 4.24: Case 3: Power consumed by prosumers w/o PV Generation dip and HOEP spike

Fig.4.4, Fig.4.8, and Fig.4.17. This low cost period is essential for prosumers as it allows them to store energy in preparation of an unexpected occurrence or for expected future system states. Another thing to note is the participation of prosumers in the P2P market for energy trade and the hours during which this market operates. For the simulations containing disturbances, the P2P market operation hours can be seen in Fig.4.6, Fig.4.12 and Fig.4.21. In the absence of any unexpected deviations these same simulations show slightly different operations, as shown in Fig.4.13 and Fig.4.22. From these figures we can conclude that the prosumers tend to engage in P2P energy trade at hours when the PV generation is significant and/or when the grid power price is sufficiently high.

The prosumers' ESS is an essential facility for many of the strategies employed to achieve optimal operation for the developed market objectives, as discussed earlier. There are however, some limitations that can be inferred from the prosumer SOC plots. Note that in all the simulations experiencing an HOEP spike, the prosumer SOC plots indicate maximum discharging at the hour of the spike (Fig.4.8 and Fig.4.17). This power is discharged by prosumers to meet their self-demand, and for sale in the P2P market in order to minimize their gird power purchase at that hour. This is only effective to a certain extent as seen in Fig.4.10 and Fig.4.19 where only some prosumers manage to reduce their grid

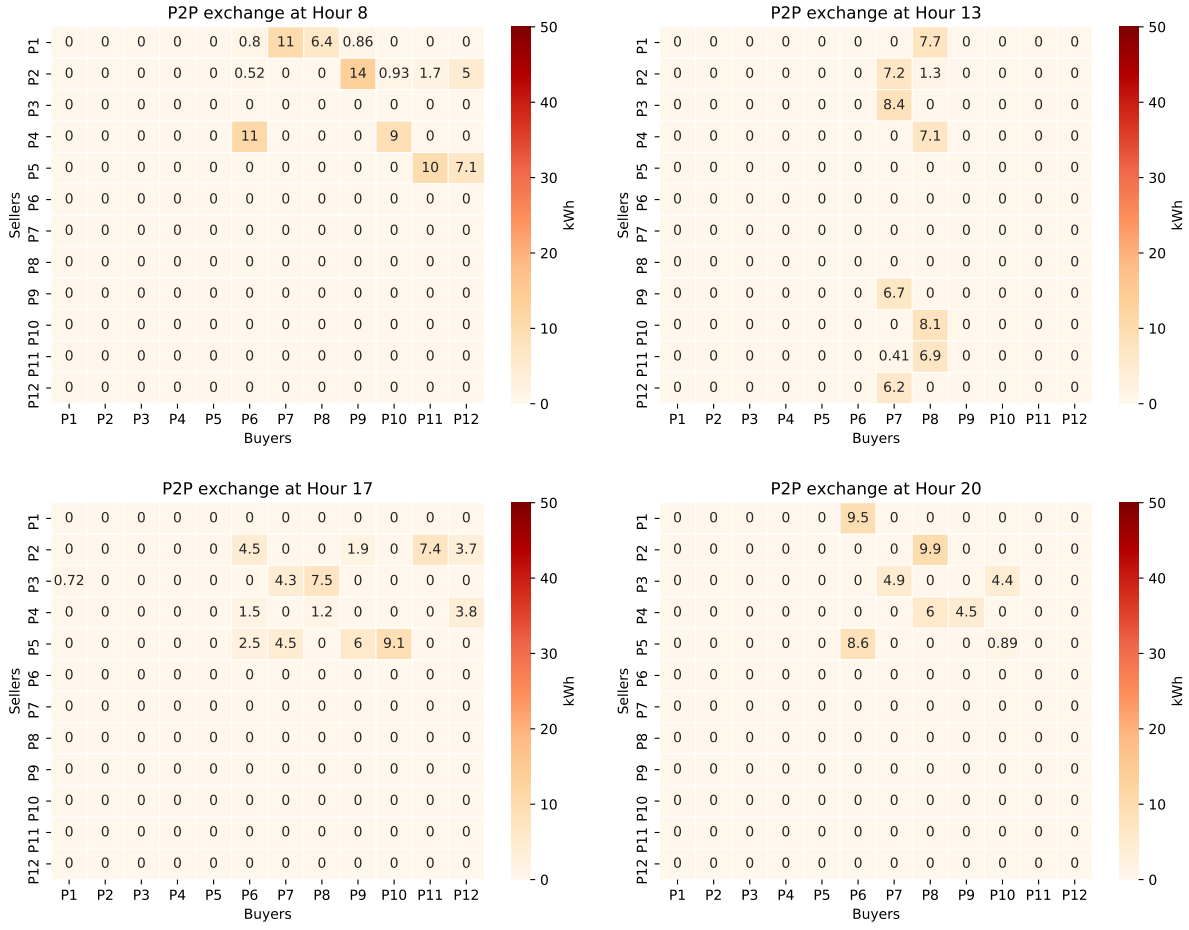

Figure 4.25: Case-3: Notable heatmaps for P2P exchange

power purchase to zero. The majority of prosumers are only able to reduce this purchase to some degree. In this case, the maximum ESS discharge limit ($P_i^{Dch_{\max}}$) is the bottleneck in the system since a higher discharge power limit would have increased the amount of power available for sale in the P2P market at Hour 20. Similarly when charging early in the day the maximum ESS charging limit ($P_i^{Ch_{\max}}$) restricts the amount of low cost energy that can be stored, for use during hours with higher cost of power.

The strategies employed by the prosumers for a particular market objective are generally separated by analyzing the trends. In a particular trend however (e.g. low consumption at high grid power price, charging the ESSs at low grid power price) the exact prosumer response depends on the utility function parameters ($\alpha_{i,t}$,β_i) selected for that prosumer. Hence these parameters must be selected carefully if the behavior of prosumers in a system with MPC based control needs to be fine tuned.

4.4 Summary

In this chapter an MPC based approach was developed and implemented on the Multi-layer P2P energy trading framework formulated in the previous chapter to examine the impact of various uncertainties. The objective function in the context of forecasted and actual values, was discussed along with the usage of the developed model as a 'black box'. An algorithm was then described for the application of the MPC approach with pre-generated simulation data, with instructions on how to modify it for real-time operations.

Combinations of both known and unknown uncertainties were used to develop simulation cases so that the strategies employed by prosumers could be analyzed in depth. However, only the welfare maximization objective was used in these simulations, since it reflects the most likely setting of an actual prosumer operating in such a system. The results demonstrated how the prosumers were enabled to respond dynamically to unexpected disturbances in the system while maintaining their market objective. These results were also used to identify some bottlenecks in the model parameters which were restricting the prosumers ability to employ certain strategies.

Chapter 5

Conclusion

5.1 Summary

In this thesis a comprehensive mathematical model is presented that determines the optimal decisions of prosumers with DERs in a physical electrical network. The focus of this model is multilateral and places emphasis on unconstrained prosumer operation and adherence of P2P energy trades to physical network constraints; hence it is referred to as a Multi-Layer Framework. The necessity for such a model arises from the requirements of practical realization of prosumers in a smart grid; requirements that are not addressed in the majority of literature on the topic, which instead focuses on the financial aspects of energy exchange. The background on the major components of the model is discussed in Chapter 2. The mathematical modeling of the Multi-Layer framework is presented in Chapter 3, along with the simulation results that demonstrate the various strategies the prosumers adapt for optimal operation. This optimal operation however, does not consider uncertainties or disturbances in the parameter profiles of the system. Consequently the prosumer is unable to behave dynamically in response to system disturbances or deviations.

The limitations of the model formulated in Chapter 3 are resolved through an MPC based approach developed in Chapter 4. The prosumers are simulated in an environment that provides uncertainty in either PV generation, grid power price, or both these parameters simultaneously, with the welfare maximization objective to direct their behavior. The considered uncertainties comprise of forecasting errors and unexpected system disturbances which are referred to in this thesis as 'known' and 'unknown' uncertainties respectively. The simulation results show how the prosumers behave dynamically and cohesively as a group to maximize their collective welfare when facing such uncertainties.

The following notable conclusions can be drawn from the results obtained in this thesis:

- Prosumers can participate in P2P energy exchanges even in the absence of distributed generation, provided that they have an ESS. Effectively proving that prosumer operation should be unconstrained for it to be optimal.
- P2P energy exchange increases when prosumers' generation and storage capabilities vary, i.e. majority of the observed P2P exchanges are between the prosumers with ESS and those without it.
- Prosumers can be effective at offering grid support functions if their objective is developed as such.
- Fixing the ESS starting and ending SOC over an optimization horizon can restrict certain prosumers' strategies for optimal operation.
- A low energy price 'off-peak' period is crucial for prosumers to be able to charge their ESS for use through system disturbances or at times with high power prices.
- Prosumers tend to engage in P2P exchanges during system disturbances, but the choice of ESS parameters can present bottlenecks in the system and should be carefully selected.

5.2 Contributions

The main contributions of the research presented in this thesis are given as follows.

- The development of a novel Multi-Layer P2P energy trading framework that enables prosumers to behave dynamically in a system and allows them to participate in the P2P energy market with full operational freedom of their internal resources. Several objective functions are formulated to direct prosumer behavior and the results demonstrate the benefits of this framework when improving prosumer welfare or grid operational performance.
- The proposed P2P energy trading framework includes a number of modifications for generic ESS models and the utility functions. The circular boundary constraint of the ESS model and the prosumer parameter evaluation techniques for the utility function are demonstrated to be effective from the results.

- An MPC based algorithm is developed to control the Multi-layer P2P energy trading framework such that the prosumers are enabled to respond dynamically to uncertainties and system disturbances. Several simulation cases are introduced to mimic these uncertainties in system parameters, and the prosumer responses demonstrate how the the P2P exchanges are leveraged in critical situations to maintain optimal operation.

5.3 Future Work

The study presented in this thesis offers numerous avenues for future research due to the flexibility of the mathematical models developed. In Chapter 3 some objective functions are used to direct prosumer behavior in the system. These objectives can be expanded upon by considering other factors such as economic signals, ancillary services and line power flow limits, etc., to affect prosumer behavior in the grid's favor. Furthermore, in the present work, all the prosumers in a group have the same market objective. This need not be so, and different groups of prosumers with multiple objectives can also be studied within this framework. The virtual layer for P2P energy trade can also be improved to implement blockchain technologies for the financial transactions [30] to maintain prosumer privacy. The issue of optimal placement of DERs in a smart distribution system can be explored with this model to ensure that the maximum benefit from an investment in DERs can be extracted. Most importantly, among possible future directions however, is the possible application of advanced financial strategies for the evaluation of P2P exchange and pricing. This area is ripe for research since P2P financial strategies are well explored in the literature.

In Chapter 4 an MPC based approach is developed to execute the multi-layer framework of Chapter 3 with consideration to uncertainties in system parameters. In this thesis, only the PV generation and HOEP profiles were considered to be uncertain. Some other parameters that may be considered as uncertain in future studies, include prosumer demand ($D_{i,t}^{\min}$, $D_{i,t}^{\max}$) and prosumer to grid selling price (π_t^{P2G}). Moreover, all the cases developed in Chapter 4 direct prosumer behavior with the welfare maximization objective. The cost minimization and loss minimization objectives may also be considered for further studies. A real-time forecasting tool would be a major extension to this study as it is essential for the practical implementation of the proposed MPC algorithm. The development and integration of such a tool with a real-time MPC based multi-layer P2P framework, presents an excellent area for future exploration.

References

[1] S. Lavrijssen and A. Carrillo Parra, "Radical prosumer innovations in the electricity sector and the impact on prosumer regulation," *Sustainability*, vol. 9, no. 7, p. 1207, 2017.

[2] O. Abrishambaf, F. Lezama, P. Faria, and Z. Vale, "Towards transactive energy systems: An analysis on current trends," *Energy Strategy Reviews*, vol. 26, p. 100418, 2019.

[3] H. Farhangi, "The path of the smart grid," *IEEE Power and Energy Magazine*, vol. 8, no. 1, pp. 18–28, 2010.

[4] W. Tushar, T. K. Saha, C. Yuen, D. Smith, and H. V. Poor, "Peer-to-peer trading in electricity networks: An overview," *IEEE Transactions on Smart Grid*, vol. 11, no. 4, pp. 3185–3200, 2020.

[5] W. Tushar, T. K. Saha, C. Yuen, T. Morstyn, Nahid-Al-Masood, H. V. Poor, and R. Bean, "Grid influenced peer-to-peer energy trading," *IEEE Transactions on Smart Grid*, vol. 11, no. 2, pp. 1407–1418, 2020.

[6] L. Chen, N. Liu, and J. Wang, "Peer-to-peer energy sharing in distribution networks with multiple sharing regions," *IEEE Transactions on Industrial Informatics*, pp. 1–1, 2020.

[7] A. Paudel, K. Chaudhari, C. Long, and H. B. Gooi, "Peer-to-peer energy trading in a prosumer-based community microgrid: A game-theoretic model," *IEEE Transactions on Industrial Electronics*, vol. 66, no. 8, pp. 6087–6097, 2019.

[8] H. Liu, J. Li, S. Ge, X. He, F. Li, and C. Gu, "Distributed day-ahead peer-to-peer trading for multi-microgrid systems in active distribution networks," *IEEE Access*, vol. 8, pp. 66961–66976, 2020.

[9] K. Anoh, S. Maharjan, A. Ikpehai, Y. Zhang, and B. Adebisi, "Energy peer-to-peer trading in virtual microgrids in smart grids: A game-theoretic approach," *IEEE Transactions on Smart Grid*, vol. 11, no. 2, pp. 1264–1275, 2020.

[10] H. Zhang, H. Zhang, L. Song, Y. Li, Z. Han, and H. V. Poor, "Peer-to-peer energy trading in dc packetized power microgrids," *IEEE Journal on Selected Areas in Communications*, vol. 38, no. 1, pp. 17–30, 2020.

[11] J. Kang, R. Yu, X. Huang, S. Maharjan, Y. Zhang, and E. Hossain, "Enabling localized peer-to-peer electricity trading among plug-in hybrid electric vehicles using consortium blockchains," *IEEE Transactions on Industrial Informatics*, vol. 13, no. 6, pp. 3154–3164, 2017.

[12] A. Paudel, L. P. M. I. Sampath, J. Yang, and H. B. Gooi, "Peer-to-peer energy trading in smart grid considering power losses and network fees," *IEEE Transactions on Smart Grid*, pp. 1–1, 2020.

[13] S. Nguyen, W. Peng, P. Sokolowski, D. Alahakoon, and X. Yu, "Optimizing rooftop photovoltaic distributed generation with battery storage for peer-to-peer energy trading," *Applied Energy*, vol. 228, pp. 2567–2580, 2018.

[14] T. Morstyn and M. D. McCulloch, "Multiclass energy management for peer-to-peer energy trading driven by prosumer preferences," *IEEE Transactions on Power Systems*, vol. 34, no. 5, pp. 4005–4014, 2019.

[15] A. Lüth, J. M. Zepter, P. C. del Granado, and R. Egging, "Local electricity market designs for peer-to-peer trading: The role of battery flexibility," *Applied energy*, vol. 229, pp. 1233–1243, 2018.

[16] Y. Xu, H. Sun, and W. Gu, "A novel discounted min-consensus algorithm for optimal electrical power trading in grid-connected dc microgrids," *IEEE Transactions on Industrial Electronics*, vol. 66, no. 11, pp. 8474–8484, 2019.

[17] O. Jogunola, W. Wang, and B. Adebisi, "Prosumers matching and least-cost energy path optimisation for peer-to-peer energy trading," *IEEE Access*, vol. 8, pp. 95266–95277, 2020.

[18] M. Khorasany, Y. Mishra, and G. Ledwich, "Hybrid trading scheme for peer-to-peer energy trading in transactive energy markets," *IET Generation, Transmission Distribution*, vol. 14, no. 2, pp. 245–253, 2020.

[19] J. Guerrero, A. C. Chapman, and G. Verbič, "Decentralized p2p energy trading under network constraints in a low-voltage network," *IEEE Transactions on Smart Grid*, vol. 10, no. 5, pp. 5163–5173, 2019.

[20] F. Sossan, E. Namor, R. Cherkaoui, and M. Paolone, "Achieving the dispatchability of distribution feeders through prosumers data driven forecasting and model predictive control of electrochemical storage," *IEEE Transactions on Sustainable Energy*, vol. 7, no. 4, pp. 1762–1777, 2016.

[21] A. Parisio, E. Rikos, and L. Glielmo, "A model predictive control approach to microgrid operation optimization," *IEEE Transactions on Control Systems Technology*, vol. 22, no. 5, pp. 1813–1827, 2014.

[22] S. Bruno, G. Giannoccaro, and M. La Scala, "Predictive control of demand and storage for residential prosumers," in *2017 IEEE PES Innovative Smart Grid Technologies Conference Europe (ISGT-Europe)*, pp. 1–6, 2017.

[23] O. Alrumayh and K. Bhattacharya, "Model predictive control based home energy management system in smart grid," in *2015 IEEE Electrical Power and Energy Conference (EPEC)*, pp. 152–157, 2015.

[24] C. Joe-Wong, S. Sen, S. Ha, and M. Chiang, "Optimized day-ahead pricing for smart grids with device-specific scheduling flexibility," *IEEE Journal on Selected Areas in Communications*, vol. 30, no. 6, pp. 1075–1085, 2012.

[25] P. Samadi, H. Mohsenian-Rad, R. Schober, and V. W. S. Wong, "Advanced demand side management for the future smart grid using mechanism design," *IEEE Transactions on Smart Grid*, vol. 3, no. 3, pp. 1170–1180, 2012.

[26] Algarni, Ayed, "Operational and planning aspects of distribution systems in deregulated electricity markets," 2009.

[27] C. Long, J. Wu, C. Zhang, L. Thomas, M. Cheng, and N. Jenkins, "Peer-to-peer energy trading in a community microgrid," in *2017 IEEE Power Energy Society General Meeting*, pp. 1–5, 2017.

[28] M. E. Baran and F. F. Wu, "Network reconfiguration in distribution systems for loss reduction and load balancing," *IEEE Transactions on Power Delivery*, vol. 4, no. 2, pp. 1401–1407, 1989.

[29] G. Hoogsteen, A. Molderink, J. L. Hurink, and G. J. Smit, "Generation of flexible domestic load profiles to evaluate demand side management approaches," in *2016 IEEE International Energy Conference (ENERGYCON)*, pp. 1–6, IEEE, 2016.

[30] P. Siano, G. De Marco, A. Rolán, and V. Loia, "A survey and evaluation of the potentials of distributed ledger technology for peer-to-peer transactive energy exchanges in local energy markets," *IEEE Systems Journal*, vol. 13, no. 3, pp. 3454–3466, 2019.

[31] H. Almasalma, S. Claeys, and G. Deconinck, "Peer-to-peer-based integrated grid voltage support function for smart photovoltaic inverters," *Applied Energy*, vol. 239, pp. 1037 – 1048, 2019.